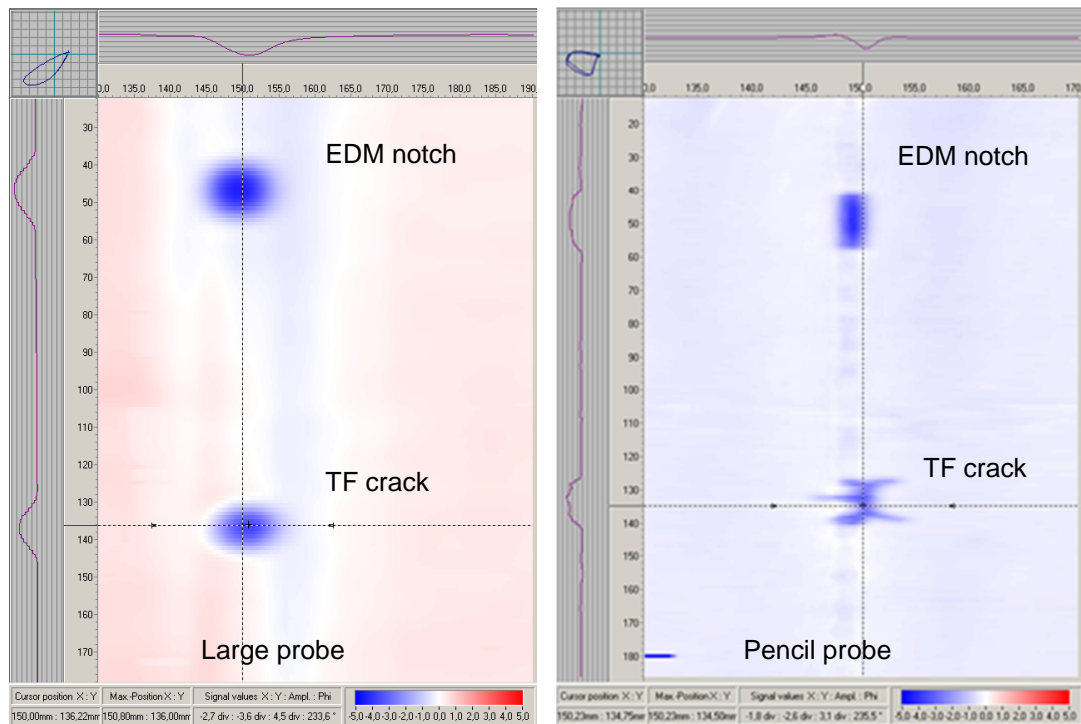






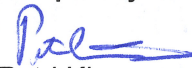
RESEARCH REPORT



Sizing of fatigue cracks using different eddy current techniques and simulation

Author: Kari Lahdenperä

Confidentiality: Public

Report's title	
Sizing of fatigue cracks using different eddy current techniques and simulation	
Customer, contact person, address	Order reference
SAFIR2018, Finnish national research program on NPP safety 2015-2018	
Project name	Project number/Short name
NDE of NPP primary circuit components and concrete infrastructure.	102177 WANDA 2015
Authors	Pages
Kari Lahdenperä	41
Keywords	Report identification code
eddy current testing (ET), mechanical fatigue crack, thermal fatigue crack, crack sizing, simulation	VTT-R-04115-15
Summary	
<p>The goal of the study was to compare the capability of different eddy current techniques in fatigue crack sizing. The effect of defect type on sizing accuracy was also to be studied. For this purpose one thermal (TF) and two mechanical (MF) fatigue cracks were manufactured. The results of destructive examination of TF and MF cracks were used to judge the capability of studied techniques and to judge applicability of the EDM notches as reference defects in crack sizing.</p> <p>Target size of the studied cracks was 5 mm (depth) x 15 mm (length). All three cracks were easily detected. TF crack had side branches. Small diameter absolute pencil probes were used in length sizing. The length sizing error was only from -0.1 mm to 0.3 mm.</p> <p>Large size probes were applied to size the depth of the cracks. Reference notches in the test pieces T284 and T285 and simulation were used to generate the family of calibration graphs. The accuracy in sizing the depth of TF crack was good. The depths of the two MF cracks were underestimated (20% - 23%). One reason for the underestimation might be the small opening of the MF cracks (3.5 µm and 2 µm) compared to the EDM notches used as reference defects. The width of EDM notches varied from 60 µm up to 440 µm depending on the depth of the EDM notch. The width of TF crack was about 60 µm.</p> <p>The depth of the EDM notch in the root area of the weld of TF piece was clearly oversized (18 %). The notch locates quite near to the middle line of the weld root. The reason for the oversizing might be the higher permeability of the weld material compared to the austenitic material of the reference pieces T284 and T285.</p>	
Confidentiality	Public
Espoo 29.9.2015	
Written by	Reviewed by
 Kari Lahdenperä Principal Scientist	 Esa Leskelä Deputy Research Team Leader
	Accepted by
	 Petri Kinnunen Deputy Head of Research Area
VTT's contact address	
VTT Technical Research Centre of Finland, PL 1000, 02044 VTT	
Distribution (customer and VTT)	
SAFIR 2018, VTT	
<p><i>The use of the name of the VTT Technical Research Centre of Finland (VTT) in advertising or publication in part of this report is only permissible with written authorisation from the VTT Technical Research Centre of Finland.</i></p>	

Preface

This report has been prepared within jointly-funded research project MAKOMON (Monitoring of the Structural Integrity of Materials and Components in Reactor Circuit) as a part of the SAFIR2014, the Finnish Research Program on Nuclear Power Plant Safety for years 2011–2014. The work has been continued in a SAFIR2018 project WANDA (Nondestructive Testing of NPP Primary Circuit Components and Concrete Infrastructure). The work was carried out at VTT Technical Research Centre of Finland. The work has been funded by the State Nuclear Waste Management Fund (VYR), VTT and Fortum Oy.

Espoo 30.9.2015

Author

Contents

Preface.....	2
Contents.....	3
1. Introduction.....	4
2. Goal.....	5
3. Description.....	5
3.1 Test pieces	5
4. Limitations	9
5. Methods.....	9
5.1 SEM examination of test pieces.....	9
5.2 Destructive examination of test pieces.....	9
5.3 Eddy current examination	9
5.4 Simulation.....	11
6. Results.....	11
6.1 Surface examination by SEM.....	11
6.2 Destructive examination.....	12
6.3 Eddy current testing.....	15
6.3.1 Send receive probe SPO-2210	15
6.3.2 Send receive probe SPO-1958	21
6.3.3 Absolute pencil probe	26
6.3.4 Differential pencil probe	33
6.4 Simulation of eddy current testing.....	35
6.4.1 Crack depth sizing with large ET probe.....	38
7. Discussion	38
8. Summary	40
References.....	41

1. Introduction

Practical trials are important part in the qualification of non-destructive examination (NDE) procedures applied in in-service inspections (ISI) of nuclear power plant (NPP) components. In practical trials test pieces with a lot of representative defects are needed. The defect shall be of similar type compared to the real service-induced defects. Cracks are typical defects detected in the components of NPP. Cracks usually locate in welds.

Service induced cracks are initiating and growing due to thermal or mechanical loading or due to corrosion (stress corrosion cracks). Fatigue cracks can be fabricated by loading the location of the intended defect thermally or mechanically. The fabrication of thermal fatigue cracks (TFC) is well controlled in respect to overall length and depth of the crack and even to crack opening. Mechanical fatigue is widely used to fabricate the mechanical fatigue cracks (MFC) for the qualification of non-destructive examination (NDE) procedures.

Notches fabricated by electro discharge machining (EDM) or by mechanical machining are routinely used as reference defect for NDE. The aim of this study was to study sizing of the cracks fabricated by thermal loading and mechanical loading and sizing of notches fabricated by EDM by eddy current method. All relevant NDE methods and techniques were used to detect, to size and to characterize the cracks before destructive examination. The applied methods included: penetrant, computed x-ray tomography and digital radiography, conventional ultrasonic, phased array ultrasonic, SEM microscopy and eddy current, see references 1 - 9. Eddy current simulation was used to extend the family of "calibration graphs" used in defect depth sizing. In this study the results of eddy current testing and eddy current simulation are given.

Eddy current techniques (ET) are sensitive to crack size and to defect characteristics like branching roughness, crack opening, tilt and skew. Eddy current techniques are also sensitive to many obstacles like the quality of the surface of the test piece, the thickness of coatings on the component, the geometry of the weld crown on the inspection surface and the permeability and conductivity of the base material and weld material. This work studies the defect sizing by practical trials and by simulation.

2. Goal

The goal of the study was to compare the capability of different eddy current techniques in defect sizing. Also the effect of defect type (TFC and MFC) on sizing accuracy was to be studied. The results of destructive examination of TF and MF cracks were used to judge the applicability of to the EDM notches as reference defects in crack sizing.

3. Description

3.1 Test pieces

There were altogether four test pieces. Two of the test pieces (T284 and 285) included only narrow EDM notches in base material. EDM notches were fabricated by Mekelex Ltd in Finland, see **Figure 1 and 2**. The TF (thermal fatigue) and MF (mechanical fatigue) pieces included butt weld, true fatigue cracks and an EDM notch, see **Figure 3**. The crack in TF piece was fabricated by Trueflaw Ltd in Finland. The EDM notch was fabricated by Mekelex Ltd. The welding was conducted by VTT. MF piece and the MF cracks were fabricated by Areva NP Uddcomb AB in Sweden, see **Figure 4**. All four test pieces were of austenitic stainless steel 316L (ASTM) plate.

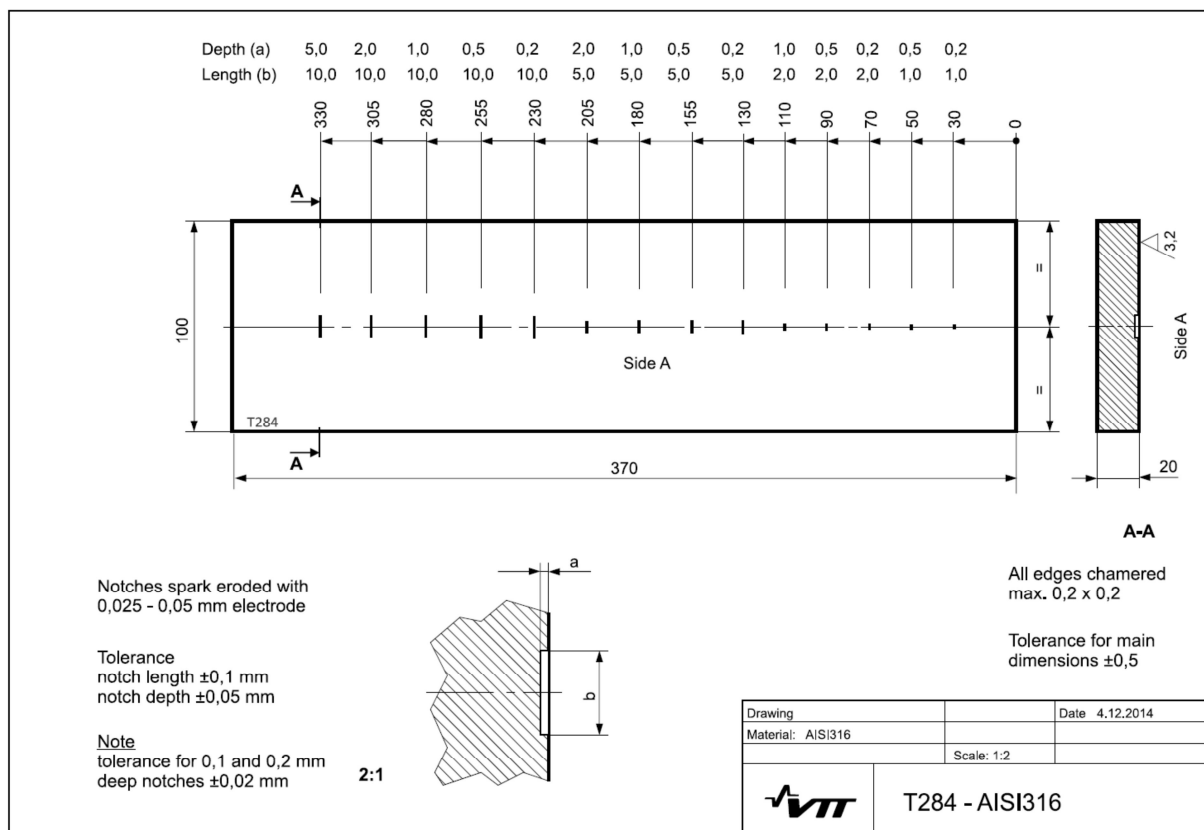


Figure 1. Test piece T284 includes 14 smaller EDM notches.

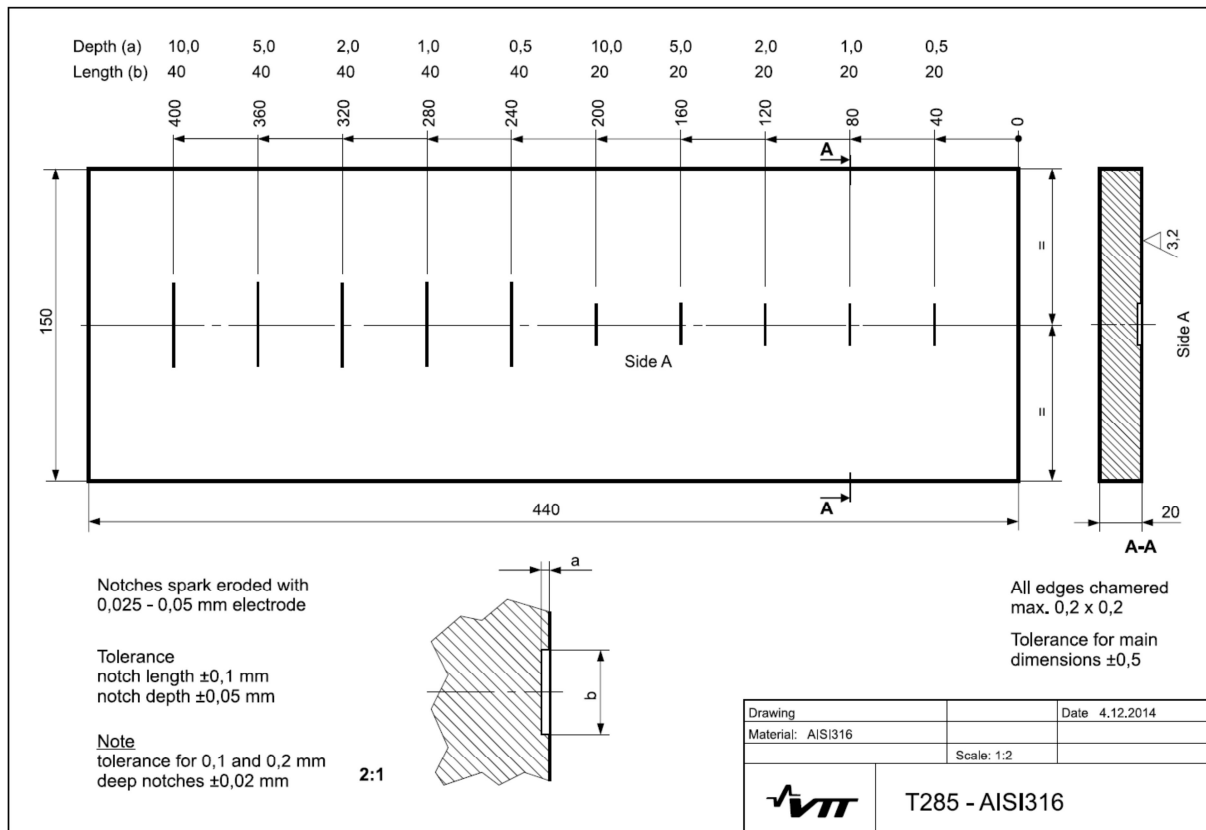


Figure 2. Test piece T285 includes 10 larger EDM notches.

The TF and MF test pieces were of similar size. There was a butt weld in the middle of both pieces. Austenitic filler metal was used. The applied welding procedures were as follows:

TF piece: metal active gas (MAG) welding, groove angle 60° , applied filler metal ESAB OK Autrod 16.32, 316LSi, diameter 1 mm.

MF piece: tungsten inert gas (TIG) welding + shielded metal arc welding (SMAW), groove angle 60° , applied filler metal ESAB OK 16.32 and ESAB OK 63.30, diameters 2 – 3.2 mm.

The cracks and one EDM notch were fabricated on root side of the welds. The cracks and EDM notch were parallel to the weld and located in the solidification line of the weld to simulate surface breaking service induced cracks. In the TF piece there was a thermal fatigue crack and an EDM notch, see **Figure 3**. In the MF piece there were two MF cracks (MFA and MFB), see **Figure 4**. After fabrication the face and root side of the welds were ground to be able to scan across the weld and to decrease indications due to rough weld root and crown. The weld crown and root were completely removed in the grinding. After grinding the crown and root side of the weld were below the surfaces of the base material, see the lower part of **Figure 3 and 4**.

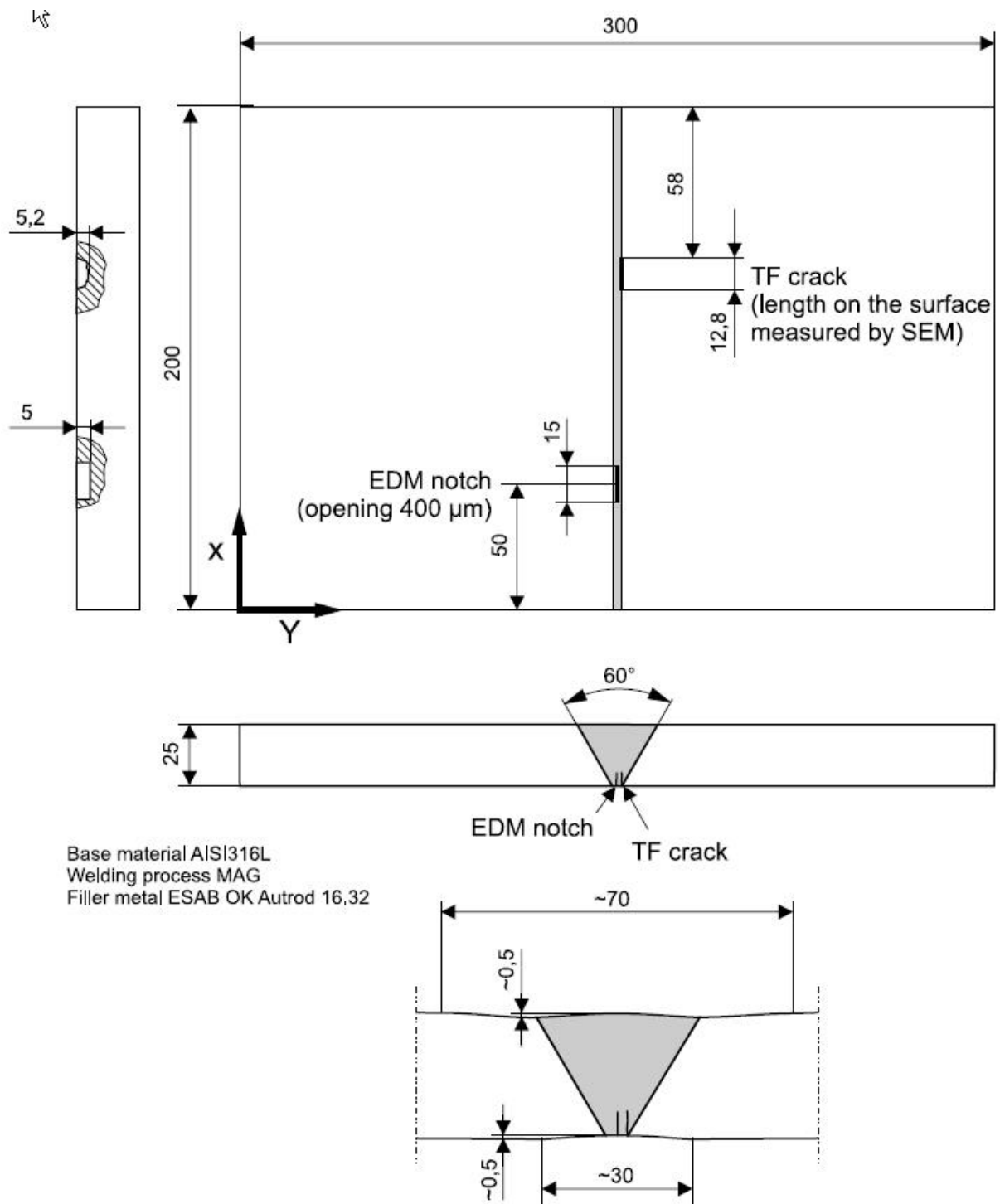


Figure 3. Drawing of TF test piece and location of fabricated TF crack and EDM notch.

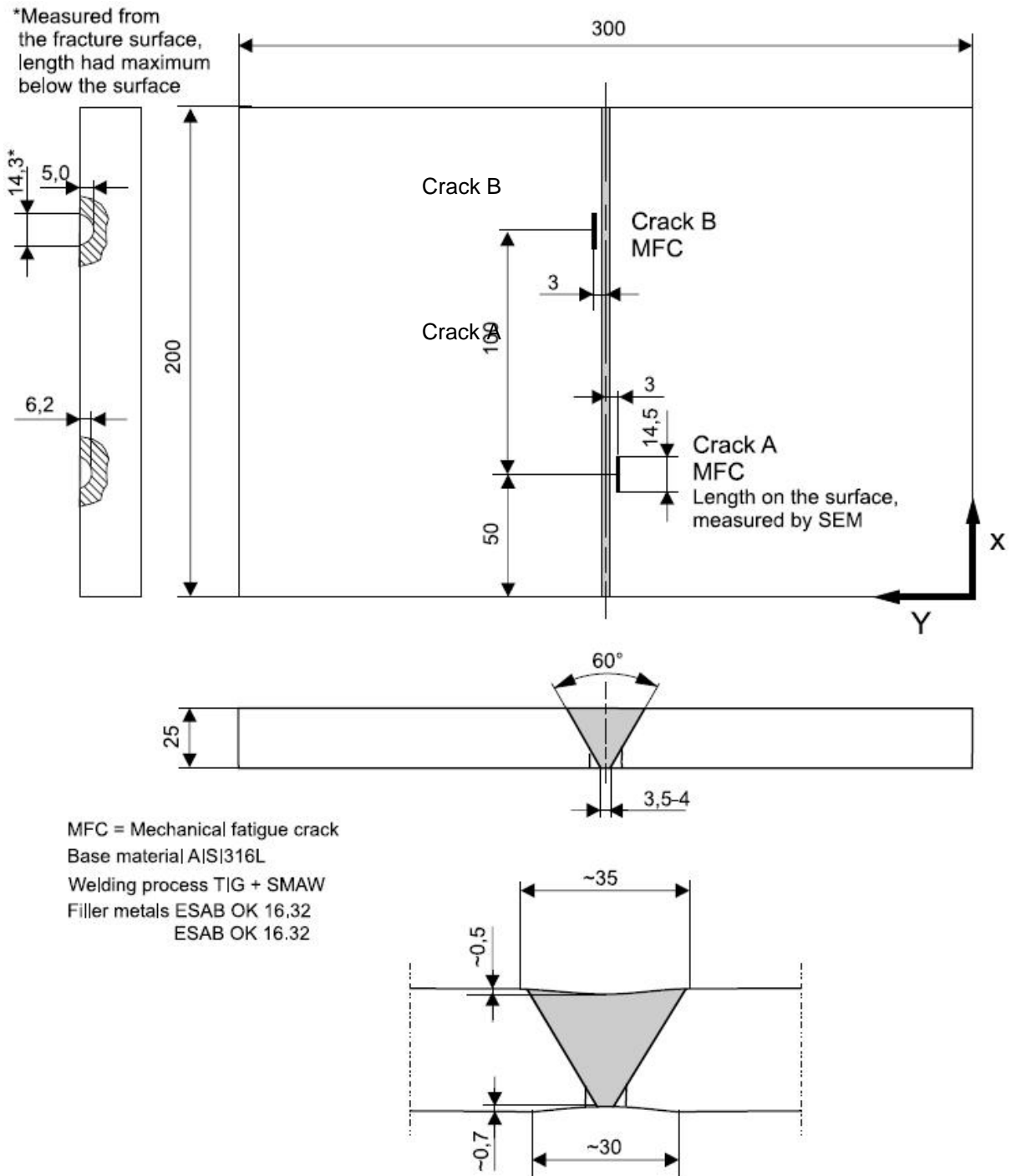


Figure 4. Drawing of MF test piece and location of fabricated MF cracks.

Liquid penetrant indications of the fabricated defects are shown in **Figures 5 a and b**. The TF crack has several branches. MF crack is straight without any branches or any other anomalies.

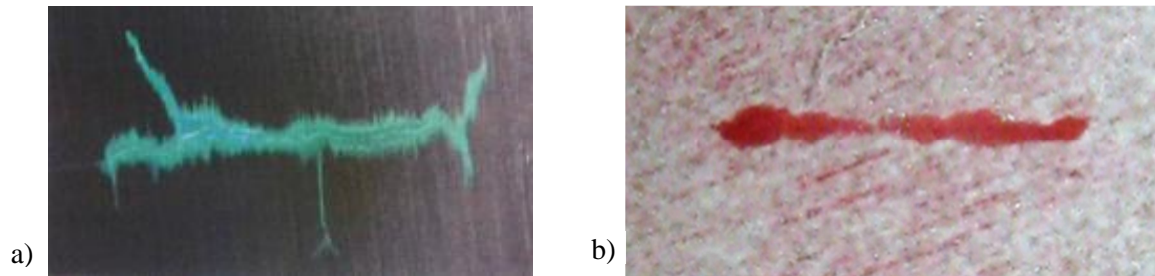


Figure 5. Liquid penetrant indications

a) Thermal fatigue crack in TF test piece b) Mechanical fatigue crack A in MF test piece.

4. Limitations

This report focuses on the crack sizing with eddy current method. The results achieved with ultrasonic testing radiography and destructive testing have been given in the previous VTT-research reports [1-8].

5. Methods

Nondestructive methods (ET and SEM) were applied to examine the capability of different techniques to detect and to size the fabricated TF and MF cracks. Destructive examination was used to measure the true size of the examined cracks.

5.1 SEM examination of test pieces

The surfaces of the test pieces were examined using scanning electron microscopy (SEM) to measure the length and crack opening of the studied fatigue cracks.

5.2 Destructive examination of test pieces

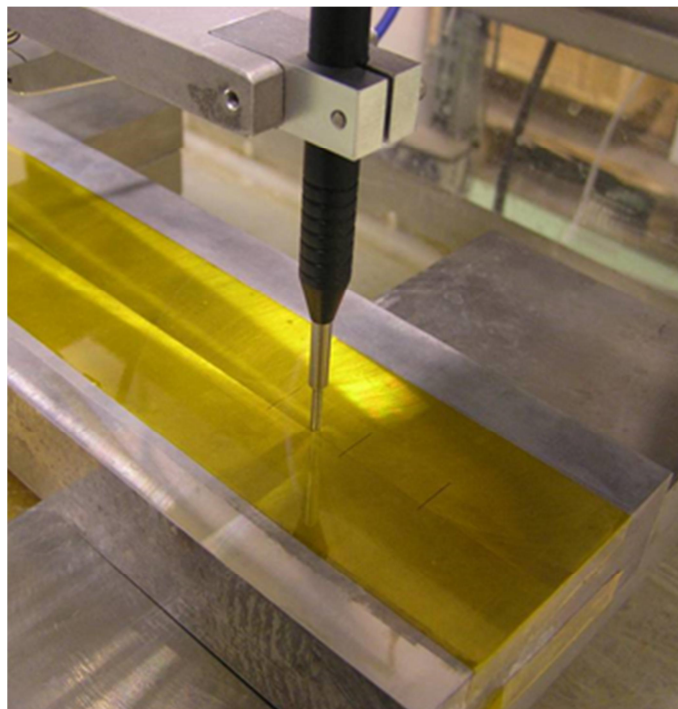
A destructive examination of all three pieces was conducted after thorough NDE and SEM examination. The cracks were opened and length and depth of the cracks were measured from stereo microscope photographs. One fracture surface of each opened crack was examined by SEM. Additionally one cross-section was cut from each sample with crack. The cross-sections of each crack were examined after polishing and etching using an optical microscope.

5.3 Eddy current examination

All four test pieces were tested with eddy current method. Mechanized scanning was used, see **Figure 6**. The cracked sides of the test pieces (root side) were scanned. Scanned area extended across the weld. The applied eddy current techniques (probes and frequencies) are shown in **Table 1** and **Figure 6**. The probes SPO-2210 and SPO1958 include two parallel axial coils side by side perpendicular to the surface to be tested. One coil is transmitter and the other is receiver. Both coils have ferrite shield. The distance between the coils of the probe SPO-1958 can be adjusted.

Table 1. Eddy current techniques used in the practical trials.

EC probe	Probe type	Probe code	Probe dimensions	Applied frequency (kHz)
SPO-2210	Axial driver and receiver coils side by side	Nortec S/N R15730 P/N 6230985	Scanning direction 19 mm Index direction 39 mm	10
				30
				100
SPO-1958	Axial driver and receiver coils side by side	Nortec S/N PO8355 P/N 9230982	Scanning direction 25 mm Index direction 45 mm	4
				10
X-probe	Differential probe, crossed tangential coils	Zetec S/N347734	Scanning direction R4 mm Index direction 8 mm	200
A-T-TS10-F4	Absolute pencil probe, internal reference coil, axial coils	EddyMax S/N 2968	Tip diameter 3 mm	100
				500
TMT DP21-02-F4	Differential pencil probe, axial coils	EddyMax S/N 2684	Tip diameter 2.8 mm	100
				500
				1200


Figure 6. Left: the large size eddy current probes (sliding coils) with separate transmitting and receiving coils. Right: small diameter pencil probe applied in scanning (photograph not from this study).

Crack depth sizing was based on amplitudes of the indication of the cracks and notches. Length sizing was based on full amplitude drop technique. The length of a defect is the distance between two end points, where the defect signal drops on the average noise level of the surrounding area.

According to ASME Code, Section XI, Appendix VIII acceptance criterion, to pass a typical weld qualification examination, the maximum difference between indicated and true state values for defect height and length is 3.18 mm and 19.05 mm, respectively.

5.4 Simulation

Program Civa 11.0 was used to simulate the eddy current indications of notches of different size (depth, length and width). Amplitudes of the simulated eddy current indications were used to complement the calibration graphs based on the amplitudes of reference defects in the test pieces T284 and T285. The measured amplitudes of the eddy current indications of the notches in test pieces were used to scale the amplitudes of the simulated indications.

6. Results

In this chapter the results of the SEM examination of the surface of the test pieces, the results of destructive examination and the results eddy current examination of the fatigue cracks are reported. For more details of SEM examination and destructive examination and radiographic and ultrasonic examination see the VTT research report VTT-R-05649-14 [1].

6.1 Surface examination by SEM

Surface examination of TF and MF pieces with SEM was conducted prior to destructive examination. Photographs of the surfaces of the test pieces MF A and TF are presented in

Figure 7, and **Figure 8**. Only minor part of the crack B on the test piece MF was visible. For this reason the length and the opening of crack B could not be determined by SEM examination.

The surface of sample MF was rather roughly ground. The crack A was straight without any branching. The opening of crack A was 3 – 4 μm . The surface length of the crack A was about 14.5 mm.

The surface of the sample TF was not so rough even if it was also ground. The mid-part of the crack was almost straight. There were V-shaped branches at both ends of the crack. There were altogether five side branches. The typical crack opening displacement of the centre part of the crack on the surface of the test piece was about of 60 μm . The measured maximum surface length of the TF crack was 12.8 mm.

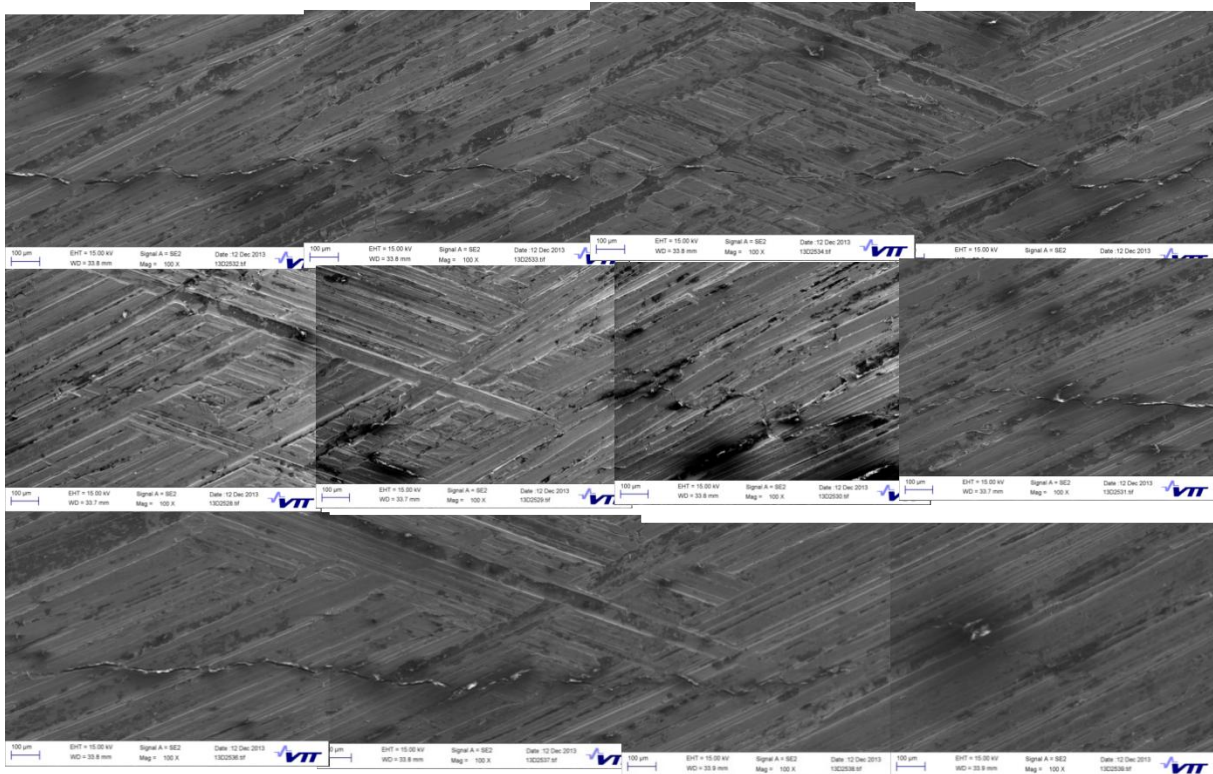


Figure 7. The surface in sample MF A. The surface has been ground. The crack is rather straight, and the length along the surface was measured to be ~14.5 mm. [1]

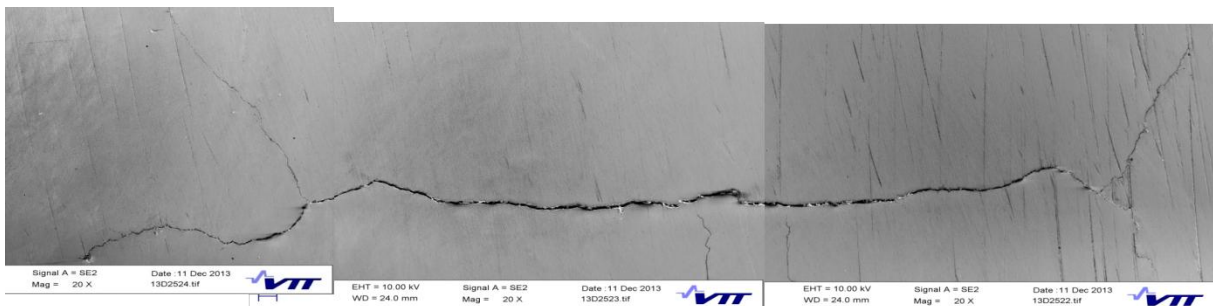


Figure 8. SEM-picture of the surface of sample TF showing the crack with V-shaped branches in both ends. The total length of the crack was measured to be 12.8 mm. [1]

6.2 Destructive examination

In the destructive examination the cracks were opened and length and depth of the cracks were measured by stereo-microscope [1]. The results are presented in **Table 2**. The photographs of the surfaces of the opened MF cracks A and B are shown in **Figure 9 and 10**. From the figures it can be deduced that the MF cracks have been “closed” by welding. SEM examination revealed that the fracture surfaces of the MF cracks were smeared. This is obviously due to hammering of the defect area after welding to make the opening displacement of the crack smaller. Hammering is necessary because the opening displacement of implanted crack is quite large after welding. The width of the weld root in the middle of the MFB crack was about 6 mm.

The photograph of the surfaces of the opened TF crack is shown in **Figure 11**. TF crack was not at all hammered or processed after thermal fatigue. Thus the fatigue striations on the

fracture surface of the unmodified TF crack were clearly seen in SEM examination. The width of the weld root in the middle of the TF crack was less than 3 mm.

As can be seen from the **Table 2** and photographs, there is a difference between the surface length of the cracks measured by SEM and maximum length of the cracks measured from the open fracture surface. The length measured from the fracture surfaces were considered more accurate. The height measurements are projections perpendicular to the surface of the test pieces. Tilt angle was not in not taken into account.

Table 2 Dimensions of the cracks in the test pieces MF A, MF B and TF [1].

Defect code	Surface length measured by SEM (mm)	Length measured from fracture surface of opened crack (mm)	Height of opened crack (mm)	Length/height
MF A crack	14.5	13.1	6.2	2.11
MF B crack	-	14.3	5.0	2.86
TF crack	12.8	13.5	5.2	2.60
Target dimensions set for manufacturers of cracks	15	5		3

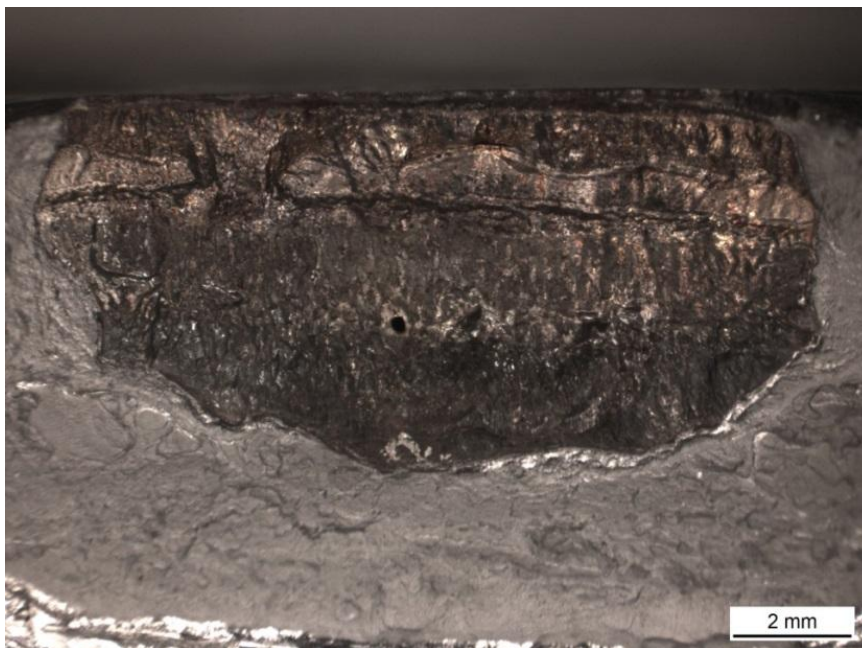


Figure 9. Photograph of the surface of the crack in test piece MF A. [1]



Figure 10. Photograph of the surface of the crack in test piece MF B. [1]

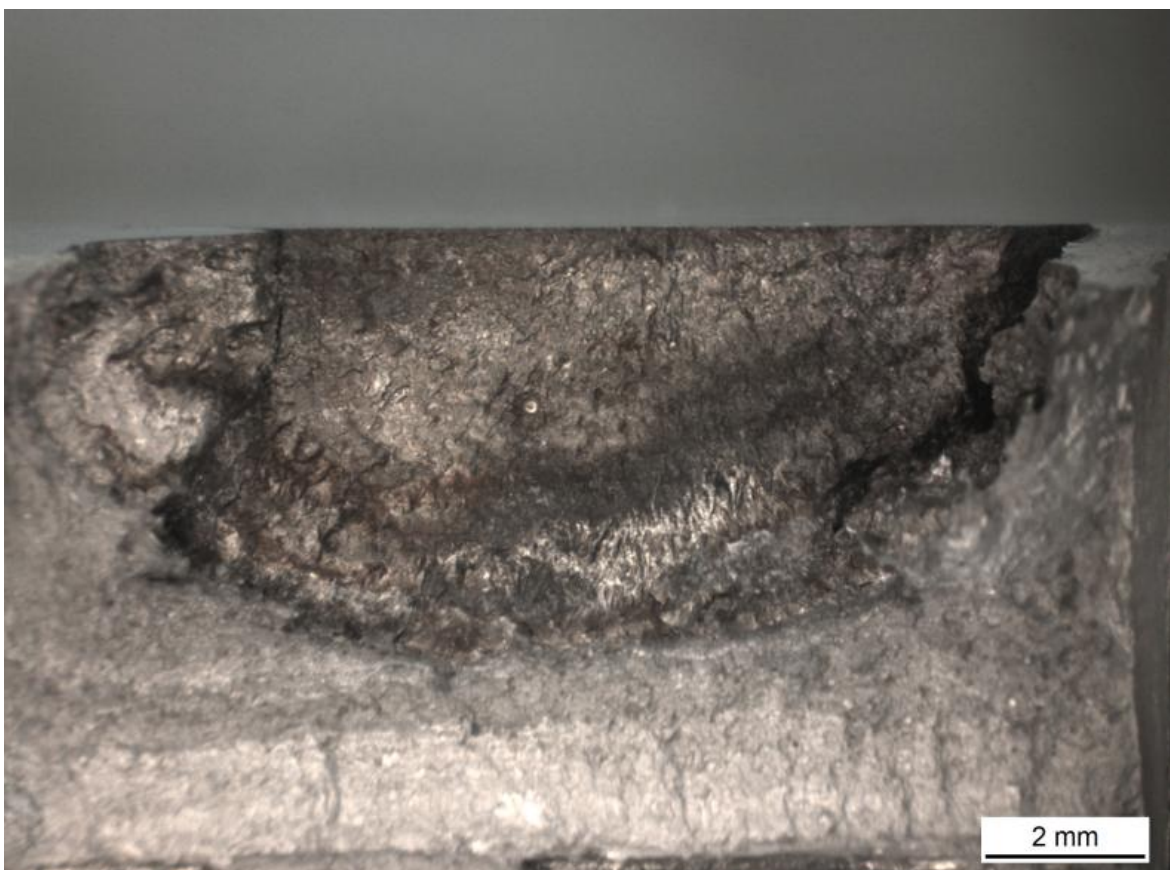


Figure 11. Photograph of the surface of the crack in test piece TF. [1]

6.3 Eddy current testing

Different ET techniques were studied. The probes used were as follows: large send-receive probe (sliding probes), x-probes and absolute probes. The applied frequencies ranged from 10 kHz up to 1.2 MHz. All results have not been reported.

The amplitudes of the indications of two deepest EDM notches in T285 (depths 5 and 10 mm) differed clearly from each other only with the large size probes SPO-2210 and SPO-1958. The indications of the cracks and the notch were also easily distinguished from the indication of weld when these probes were used.

6.3.1 Send receive probe SPO-2210

The C scans of TF and MF test pieces using 10 kHz and 30 kHz frequencies are shown in **Figures 12 and 13**. The indication of the large notch and all fatigue cracks were detected easily. The defect and weld indications have been shown in **Figure 14**. The amplitude of the smallest defect indication exceeded the typical respective weld indication at least by 7 dB. The angles of the indications of weld and defect were the same, when the frequency was 30 kHz. When 10 kHz frequency was used the angle between weld indication and defect indication was about 45°. This feature can be used to distinguish crack and weld indication in multi frequency testing.

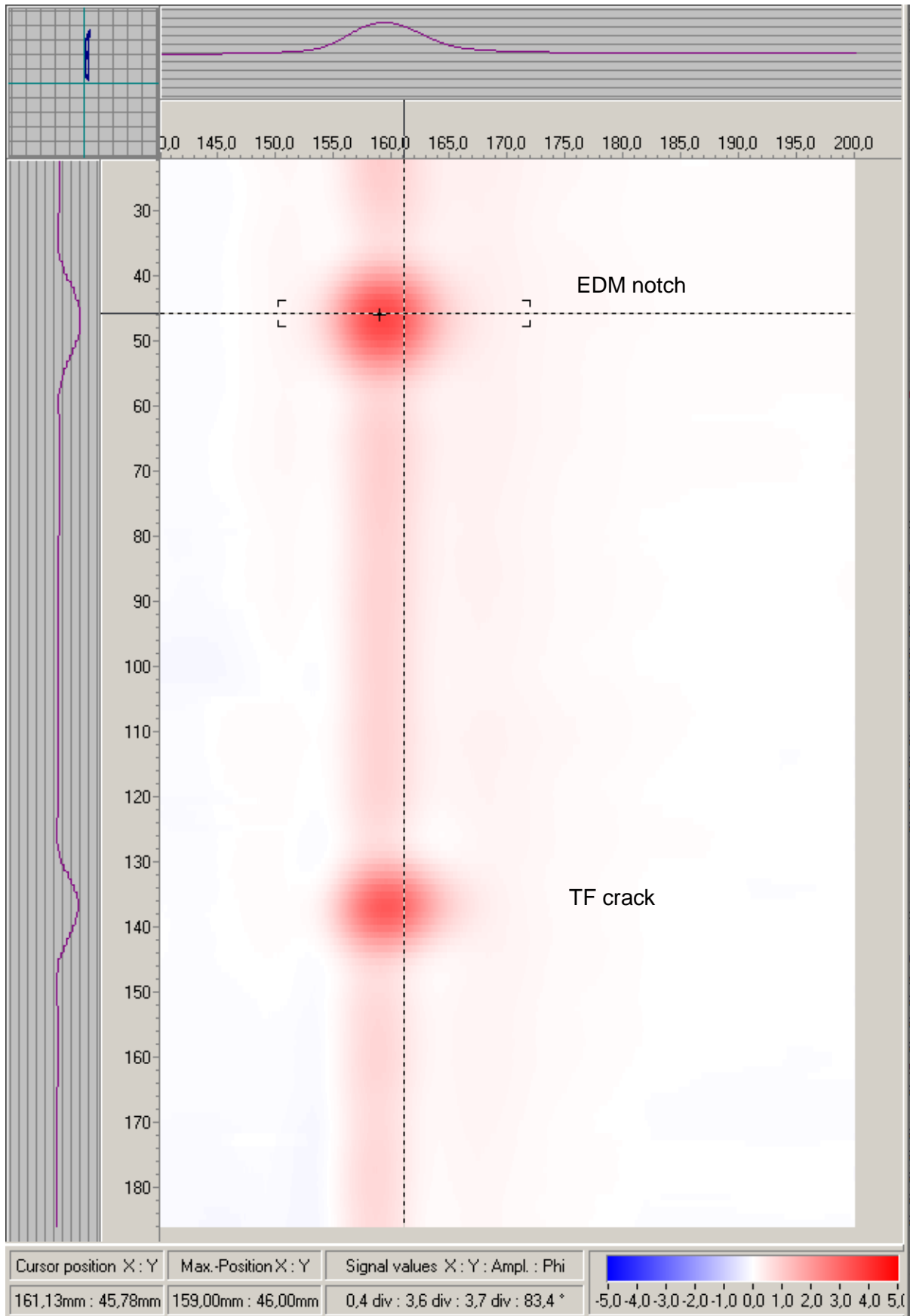


Figure 12. C scan of test piece TF, indications of a notch and a TF crack, probe SPO-2210, applied frequency 10 kHz.

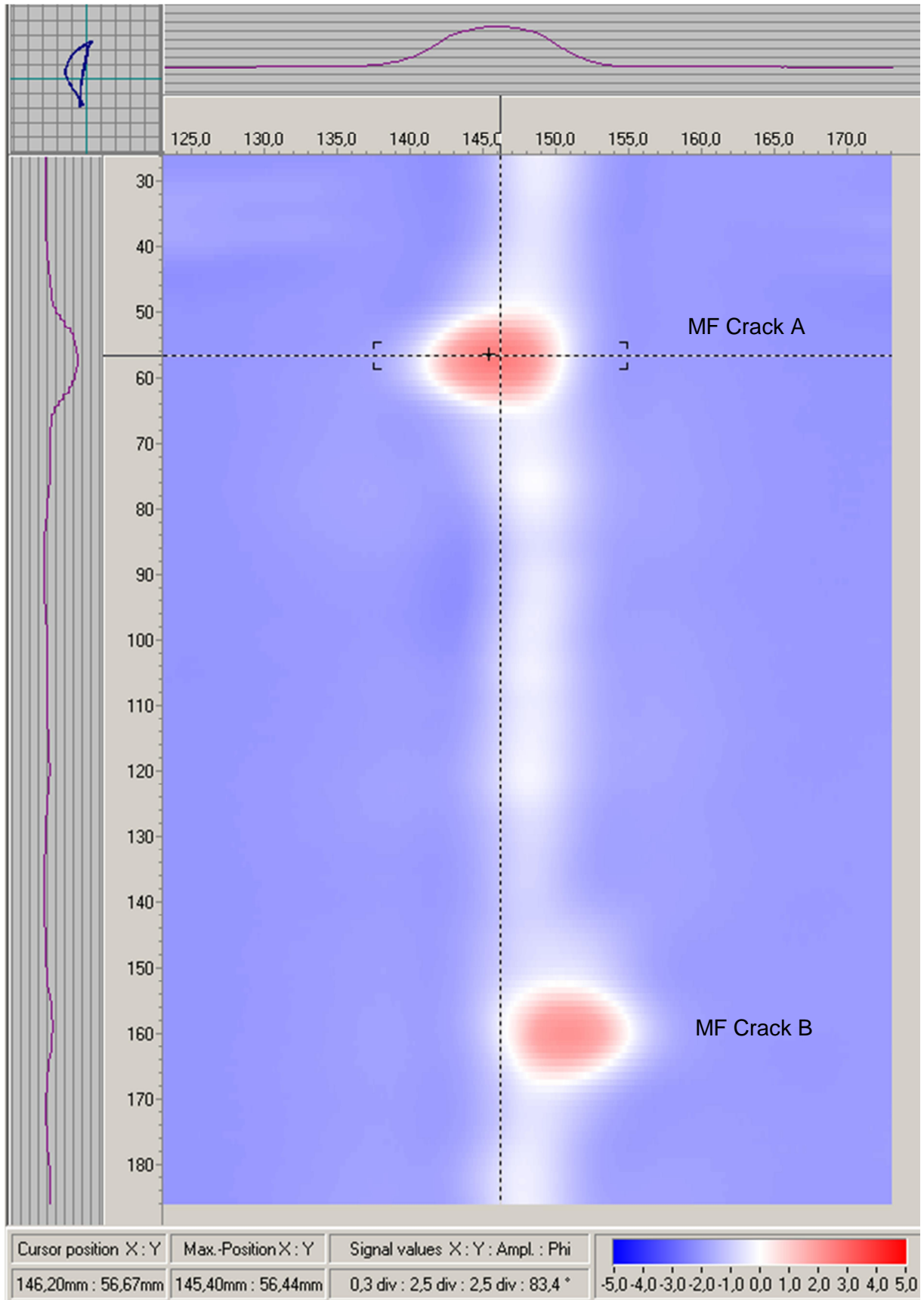
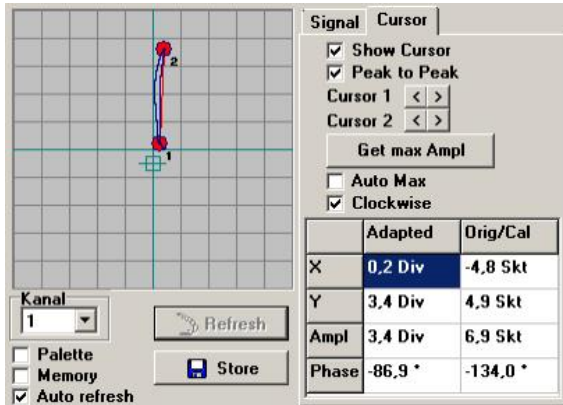
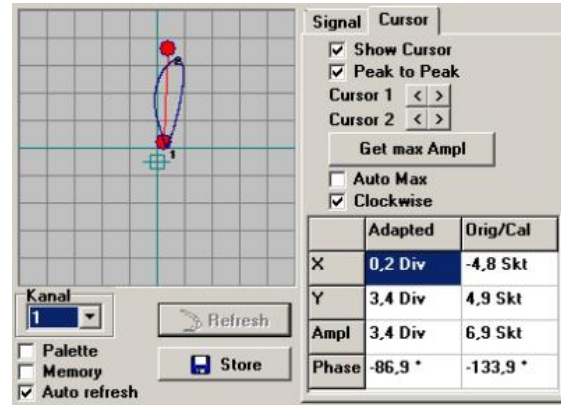


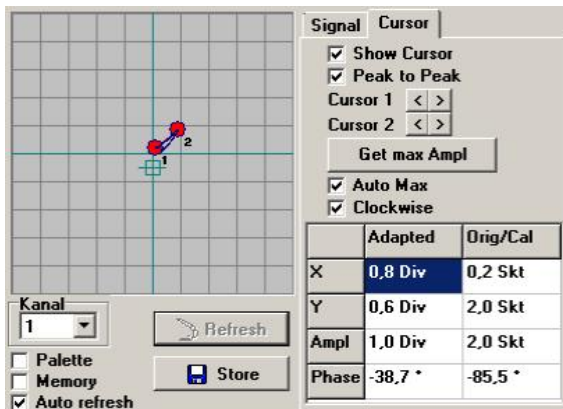
Figure 13. C scan of test piece MF, indications two MF cracks, probe SPO-2210, applied frequency 30 kHz.



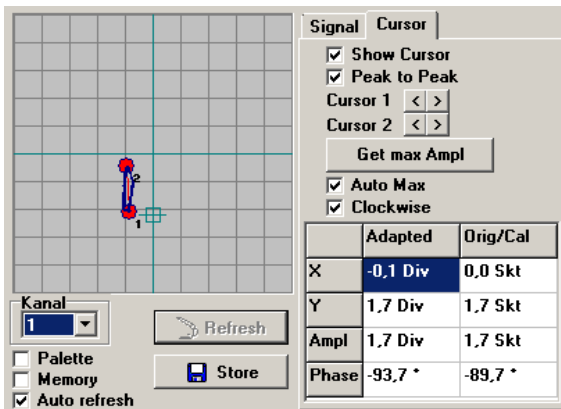
a) EDM notch, TF test piece (10 kHz)



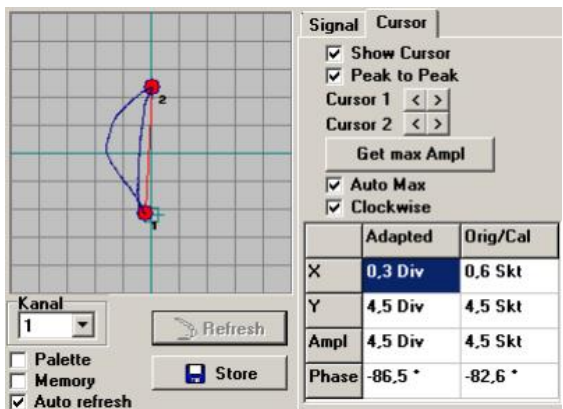
b) TF crack, TF test piece (10 kHz)



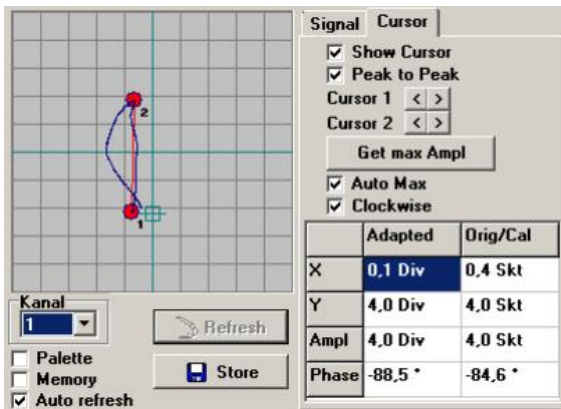
c) Typical weld indication TF (10 kHz)



d) Typical weld indication MF (30 kHz)



e) Indication of MFA crack (30 kHz)



f) Indication of MFB crack (30 kHz)

Figure 14. Impedance plane presentations of indications of a notch, fatigue cracks and welds in test pieces TF and MF, probe SPO 2210.

The amplitudes of all indications of fatigue cracks and notches of the test pieces MF, TF, T284 and T285 recorded with the smaller size probe SPO-2210 are given in **Figure 15, 16 and 17**. The applied frequencies were 10, 30 and 100 kHz. The test piece MF was tested only with 30 kHz technique. In all three cases the amplitudes of the indications of 20 mm long notches were higher than that of 40 mm long notches of equal depth. In the case of 20 mm long notch the amplitude of the indication on C scan had maximum value in the middle of the indication. In the case of 40 mm long notch the amplitude of the indication on C scan had maximum values at the ends of the indication, when the notch depth was 5 or 10 mm. The amplitude of the indication of the EDM notch (5 x 12 mm) in the weld of the TF piece was higher than that of the larger EDM notch (5 x 20 mm) in the test piece T285. When the eddy current frequency was lowest the difference between the amplitudes of these two notches was the highest. In all cases the amplitude of the indication due to this 5 mm deep and 12

mm long notch was also higher than that of the three slightly deeper and longer fatigue cracks.

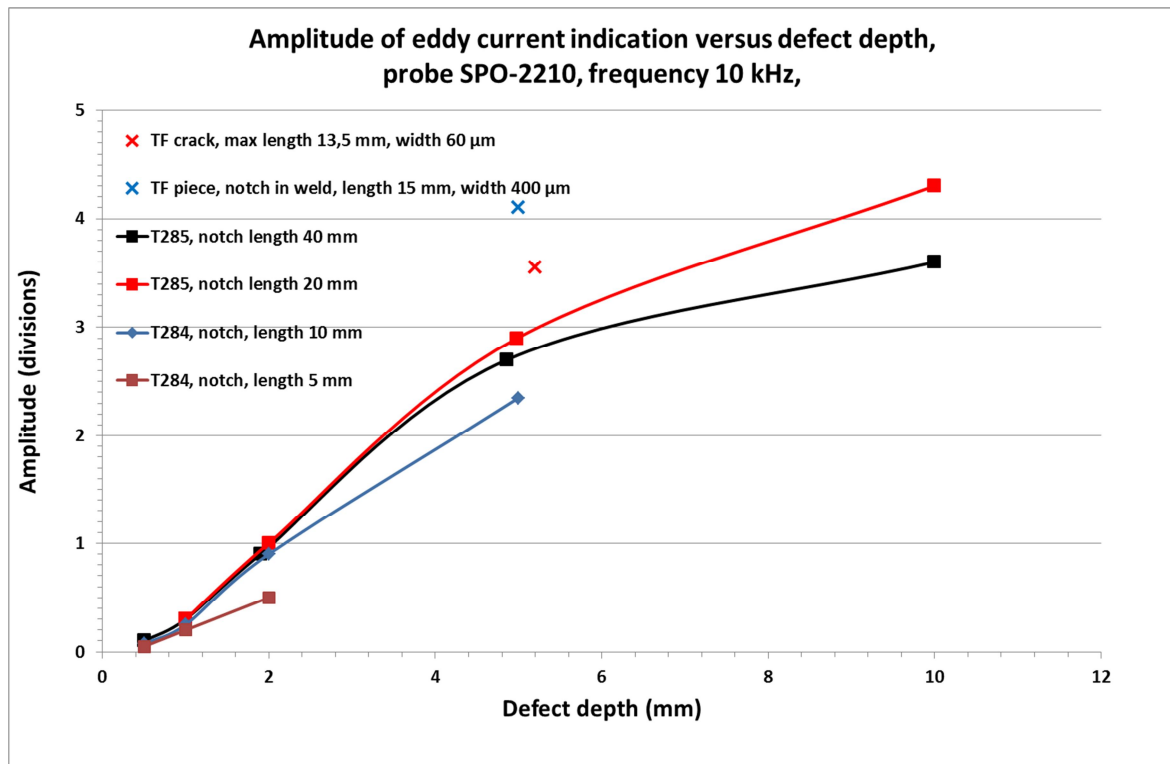


Figure 15. Amplitude of eddy current indications of TF crack and notches versus defect depth, when probe SPO-2210 was used. The studied test pieces were TF, T284 and T285. The eddy current frequency was 10 kHz.

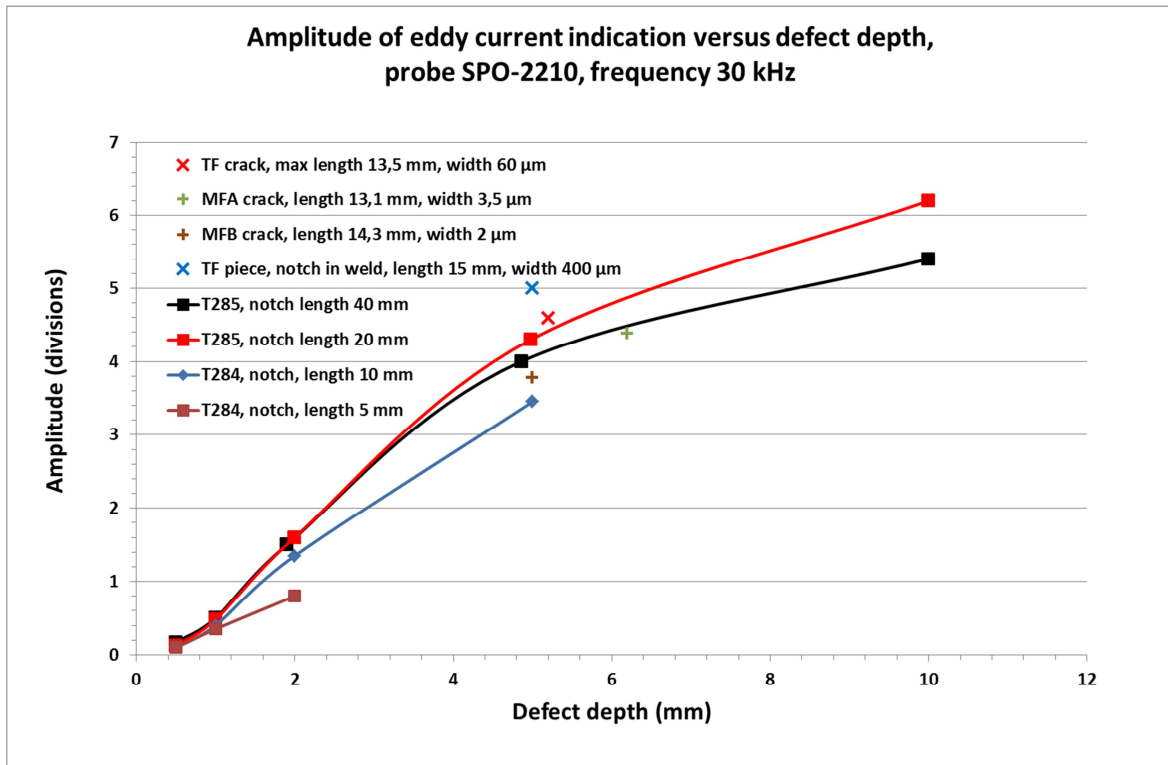


Figure 16. Amplitude of eddy current indications of TF, crack, two MF cracks and notches versus defect depth, when probe SPO-2210 was used. The test pieces were TF, MF and T284 and T285. The eddy current frequency was 30 kHz.

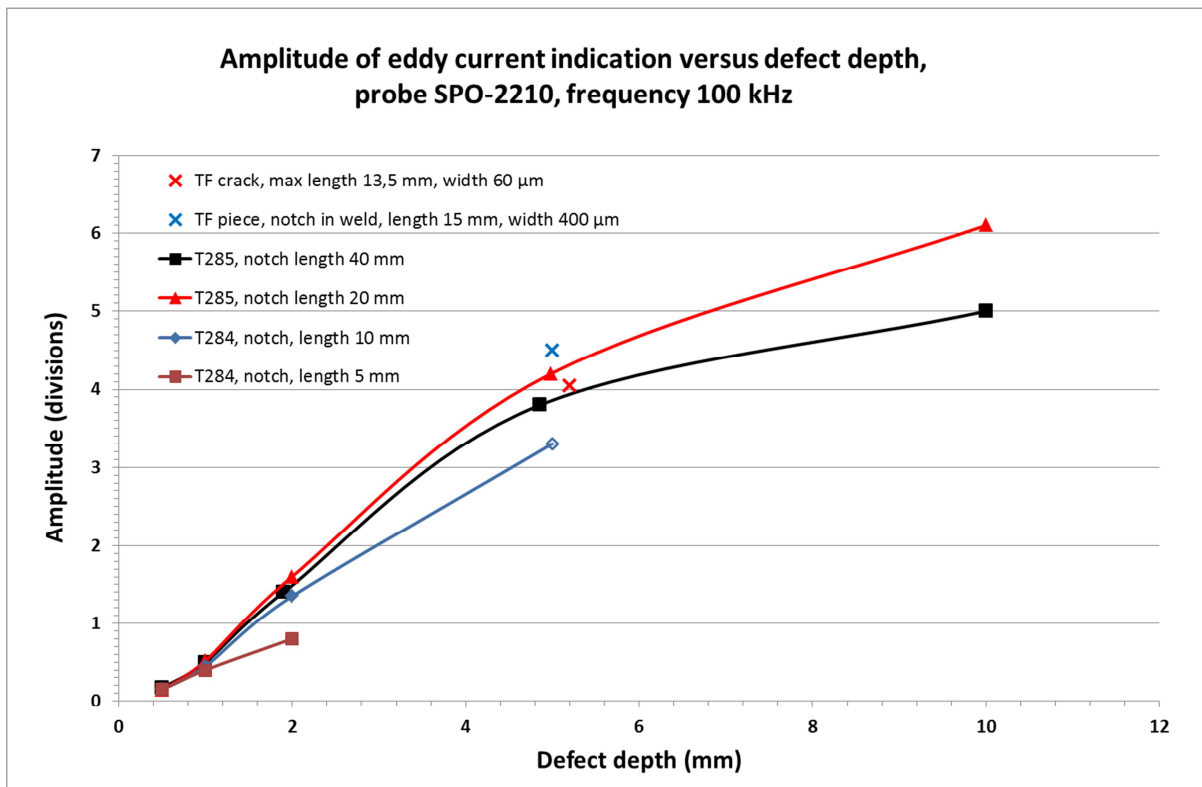


Figure 17. Amplitude of eddy current indications of TF crack and notches versus defect depth, when probe SPO-2210 was used. The eddy current frequency was 100 kHz.

6.3.2 Send receive probe SPO-1958

The amplitudes of all indications of fatigue cracks and notches of the test pieces MF, TF, T284 and T285 recorded with the probe SPO-1958 are given in **Figure 18 and 19**. The applied frequencies were 4 and 10 kHz. The test piece MF was tested only with 10 kHz technique. In both cases the amplitudes of the indications of 40 mm long notches were higher than that of 20 mm long notches of equal depth. The amplitude of the indication of the EDM notch (5 x 12 mm) in the weld of the TF piece was higher than that of the longer EDM notch (5 x 20 mm) in the test piece T285. In all cases the amplitude of the indication of this 5 mm deep and 12 mm long notch was higher than that of the three slightly deeper and longer fatigue cracks.

The amplitudes of the indications of two deepest EDM notches (depths 5 and 10 mm) differed clearly from each other only with the large size probes SPO-2210 and SPO-1958. The indications of the crack and notch indications were also easily distinguished from the weld indication when these probes were used.

1.1.1 X-probe

The C scans of TF and MF test pieces using X probe and 200 kHz frequency are shown in Figures 20 and 21. The indication of the large notch and fatigue cracks can be detected easily. The defect and weld indications have been shown in Figure 14. The amplitude of the smallest defect indications exceeds the typical respective weld indication least by 8 dB. The angles of the indications of the welds, notch and cracks were practically the same.

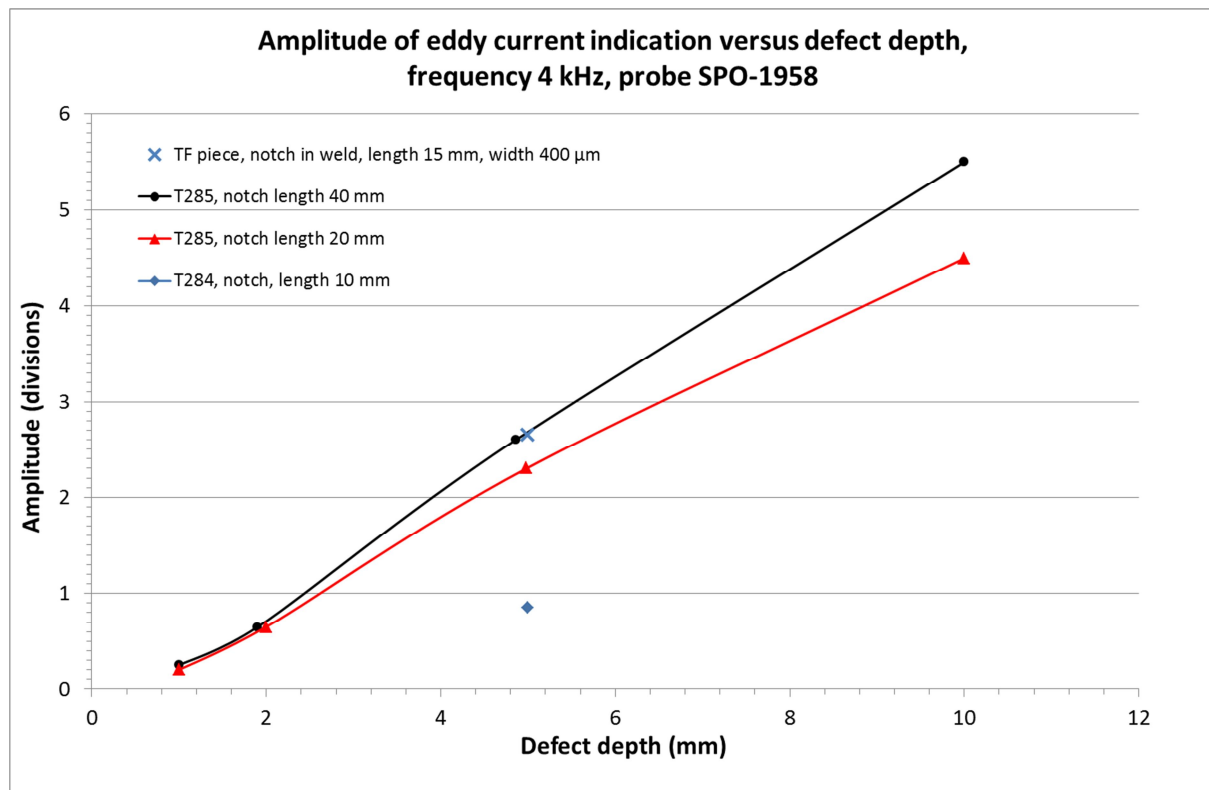


Figure 18. Amplitude of eddy current indications of EDM notches versus defect depth, when probe SPO-2210 was used. The studied test pieces were TF, T284 and T285. The eddy current frequency was 4 kHz.

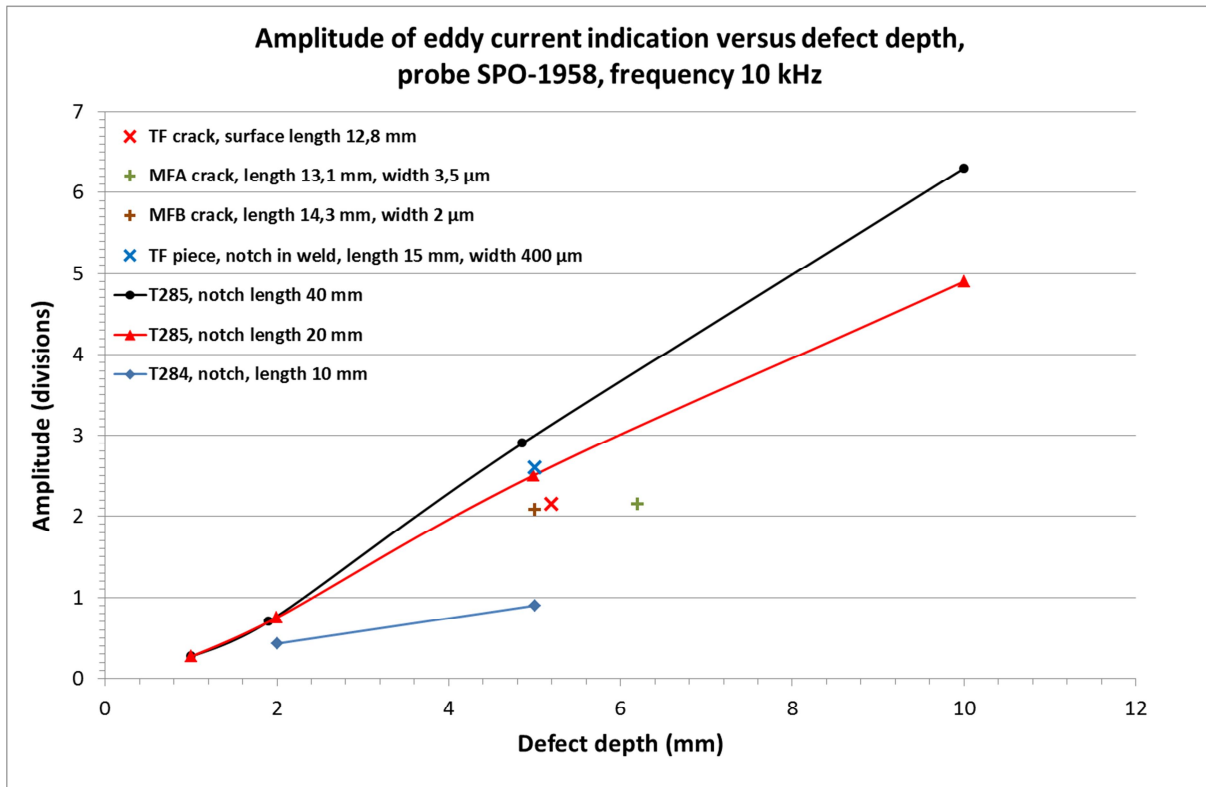


Figure 19. Amplitude of eddy current indications of TF crack and notches versus defect depth, when probe SPO-2210 was used. The studied test pieces were TF, T284 and T285. The eddy current frequency was 10 kHz.

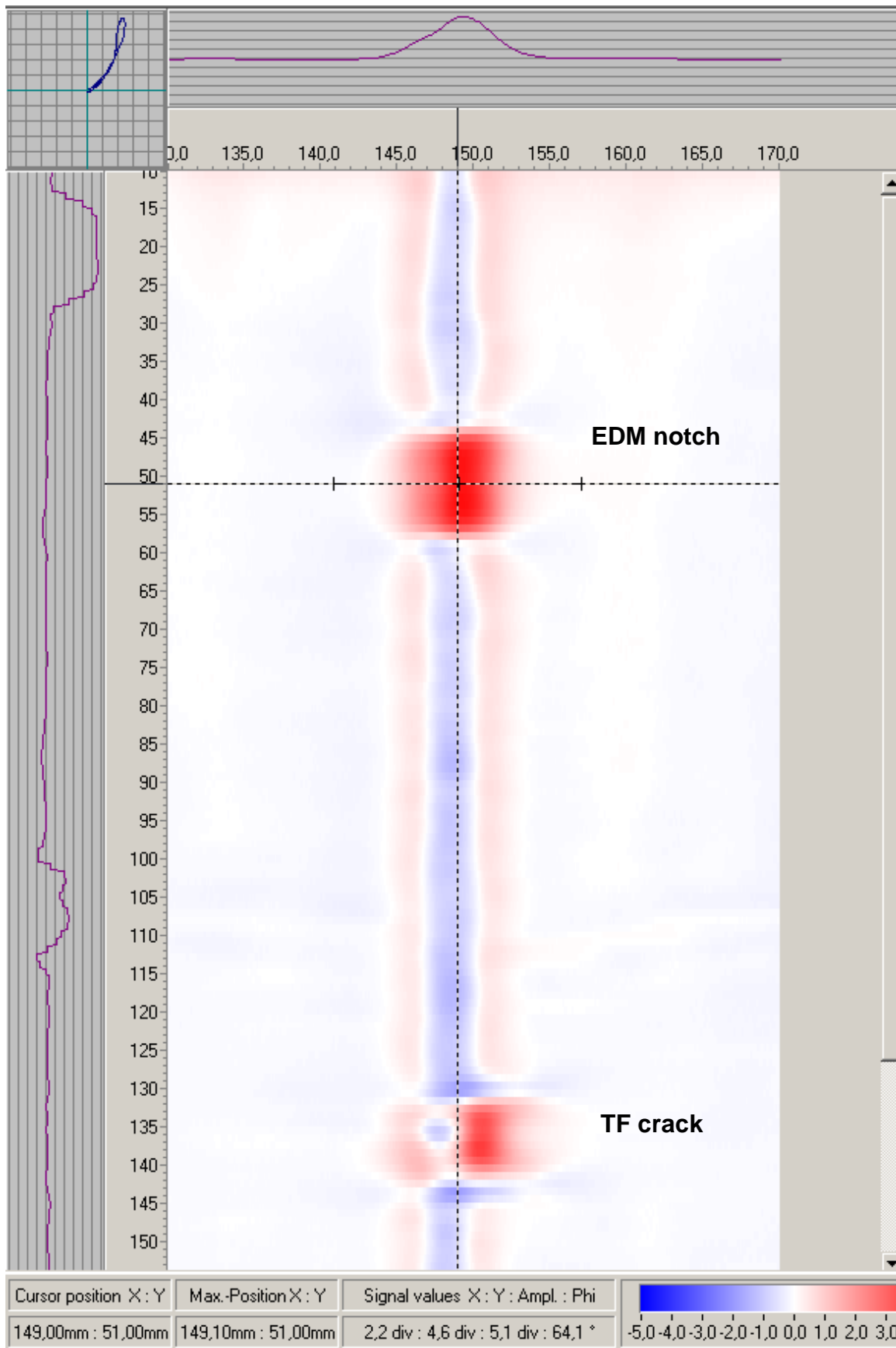


Figure 20. C scan of test piece TF, when X probe was used and the applied frequency was 200 kHz.

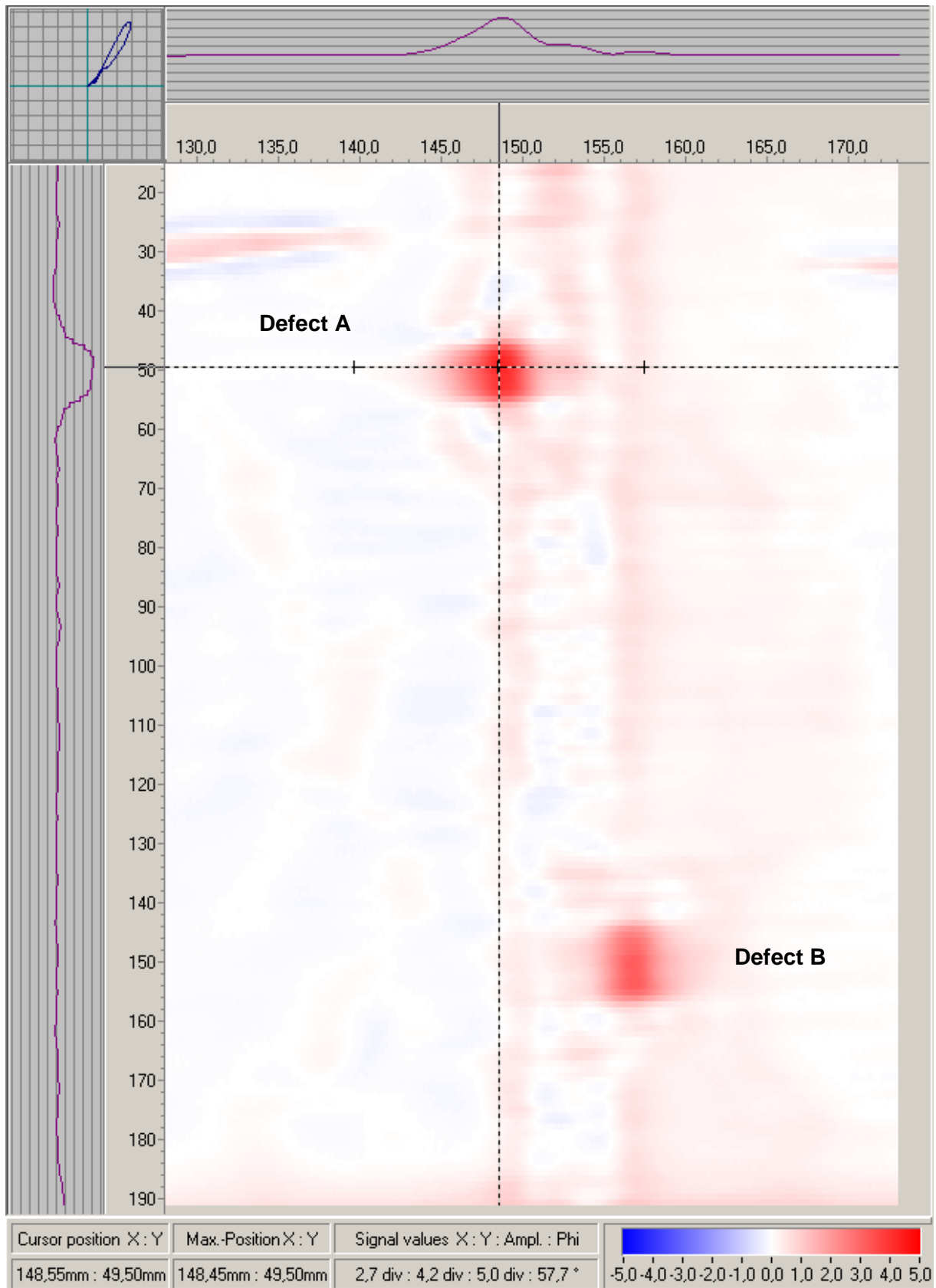


Figure 21. C scan of test piece MF, when X probe was used and the applied frequency was 200 kHz.

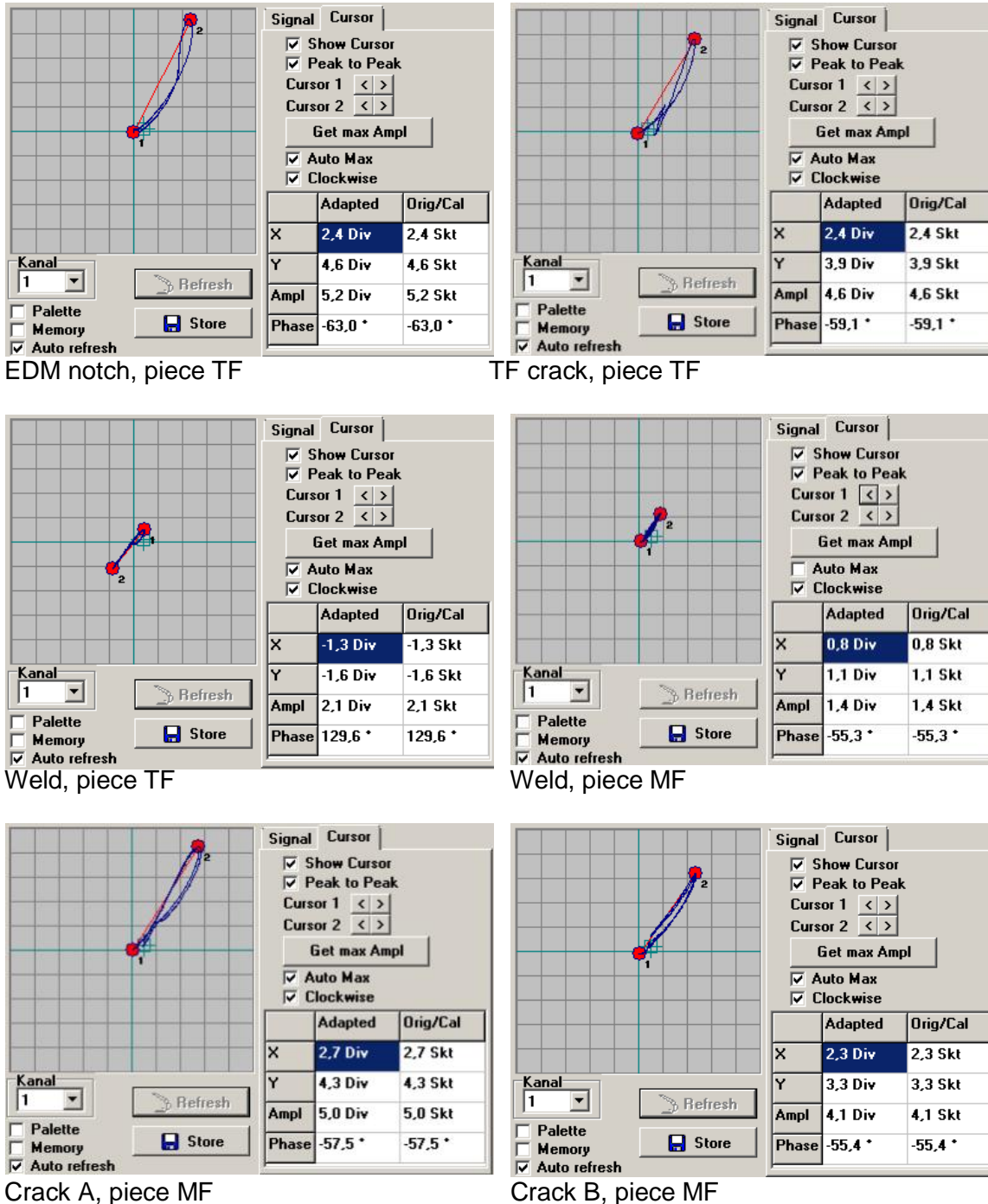


Figure 22. Impedance plane presentations of indications of a notch, fatigue cracks and welds in test pieces TF and MF, when X probe was used.

The amplitudes of all indications of fatigue cracks and notches of the test pieces MF, TF, T284 and T285 recorded with the X probe are given in **Figure 23**. The applied frequency was 200 kHz. The amplitudes of the indications of 40 mm and 20 mm long notches were practically the same. The amplitude of the indication of the EDM notch (5 x 12 mm) in the weld of the TF piece was higher than that of the longer EDM notch (5 x 20 mm) in the test piece T285. In all cases the amplitude of the indication due to this 5 mm deep and 12 mm long notch was higher than that of the three slightly deeper and longer fatigue cracks. The amplitude of the MF crack A was the highest of all crack indications. The applied technique can be used to size defect lengths, but not to size the depths deeper than 2 mm due to the increasing saturation of the amplitude of the indications when the defect depth exceeds 2 mm.

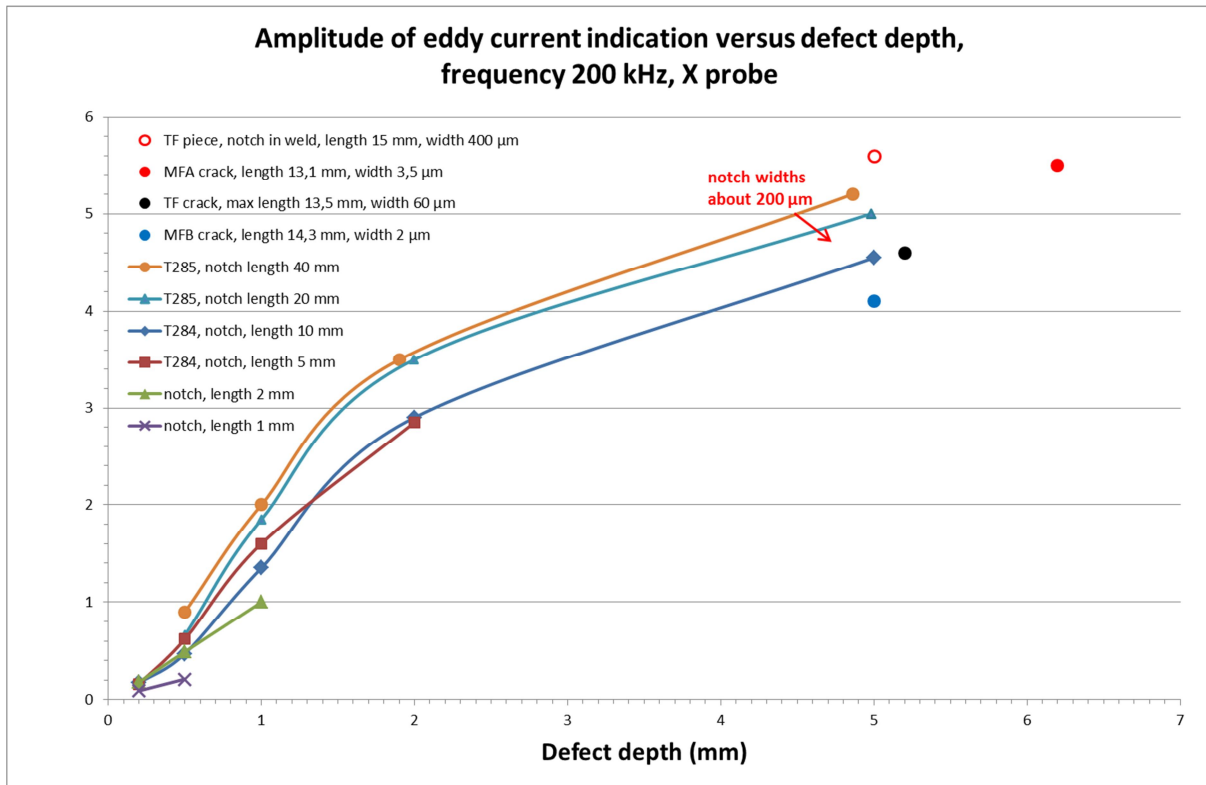


Figure 22. Amplitude of eddy current indications of TF and MF crack and notches versus defect depth, when X probe was used. The studied test pieces were TF, MF, T284 and T285. The eddy current frequency was 200 kHz.

6.3.3 Absolute pencil probe

The C scans of TF and MF test pieces using absolute probe A-T-TS10-F4 and 100 kHz frequency are shown in **Figures 23 and 24**. In the C scans of the TF piece the Y component of the recorded eddy current signal is presented. The crack and notch can be clearly seen in **Figure 23a**. Even the five side branches of TF crack can be clearly seen. The weld line can be seen well in **Figure 23b**, where 20 dB additional gain was applied.

The indications of the fatigue cracks A and B can in the MF test piece be seen easily in **Figure 24 a**. The weld line can be seen and the additional welds needed in defect fabrication and implanting can also be easily seen in **Figure 24 b**. Here the scanning direction during data acquisition was not exactly perpendicular to the weld line. For this reason the indications of the weld and defects in the C scan of test piece MF (**Figure 24 a and b**) are slightly tilted in respect to index axis (vertical axis).

The Y components of the amplitude of the smallest defect indications exceeded the maximum weld indication by 9 dB. The amplitude of the Y component of the indication of the weld was highest in the case of MF piece. The applied technique can be used to size defect length, but not to size the depths of deep defects.

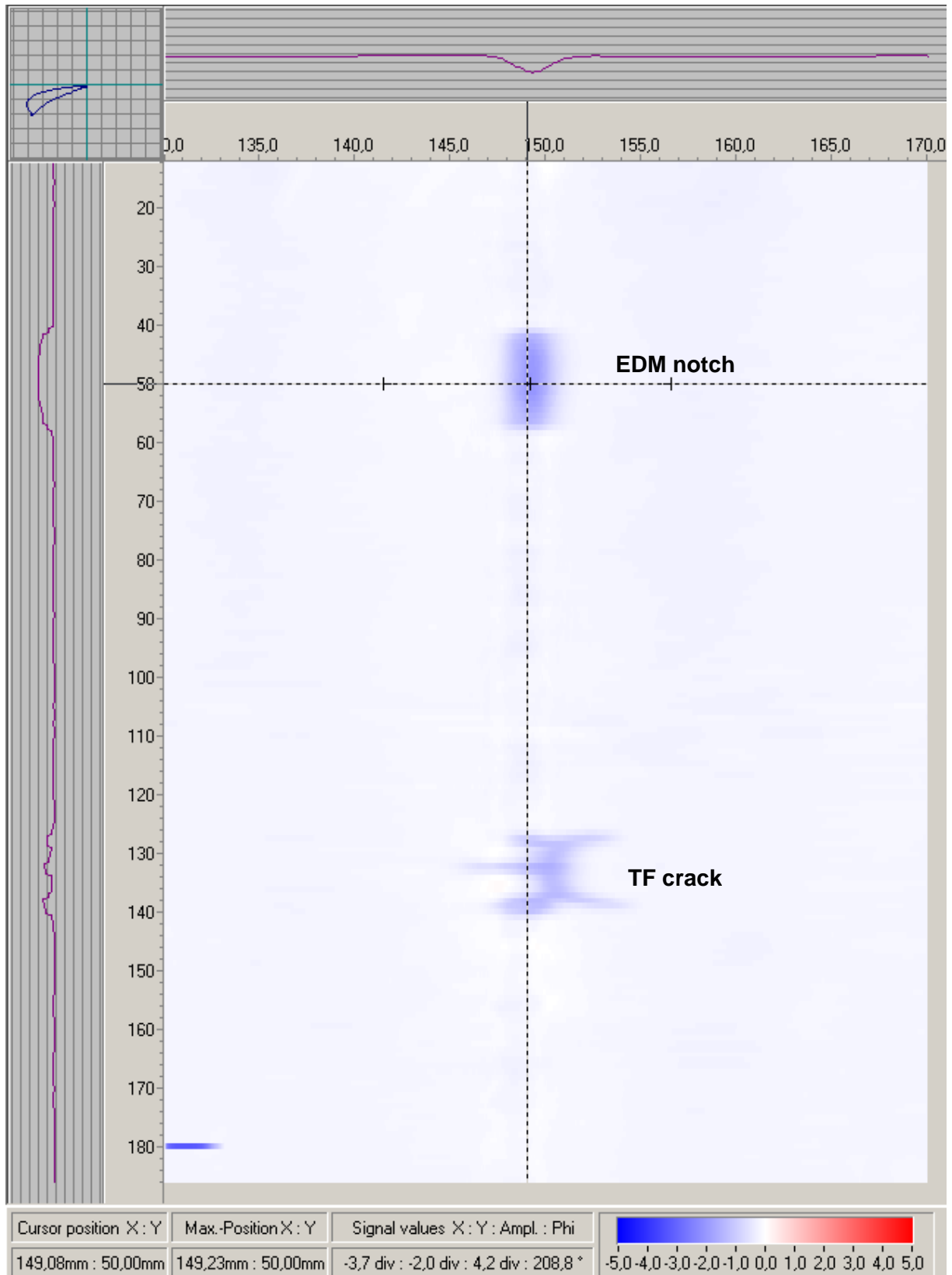


Figure 23a. C scan of the test piece TF (Y-component), small diameter absolute probe A-T-TS10-F4, frequency 100 kHz.

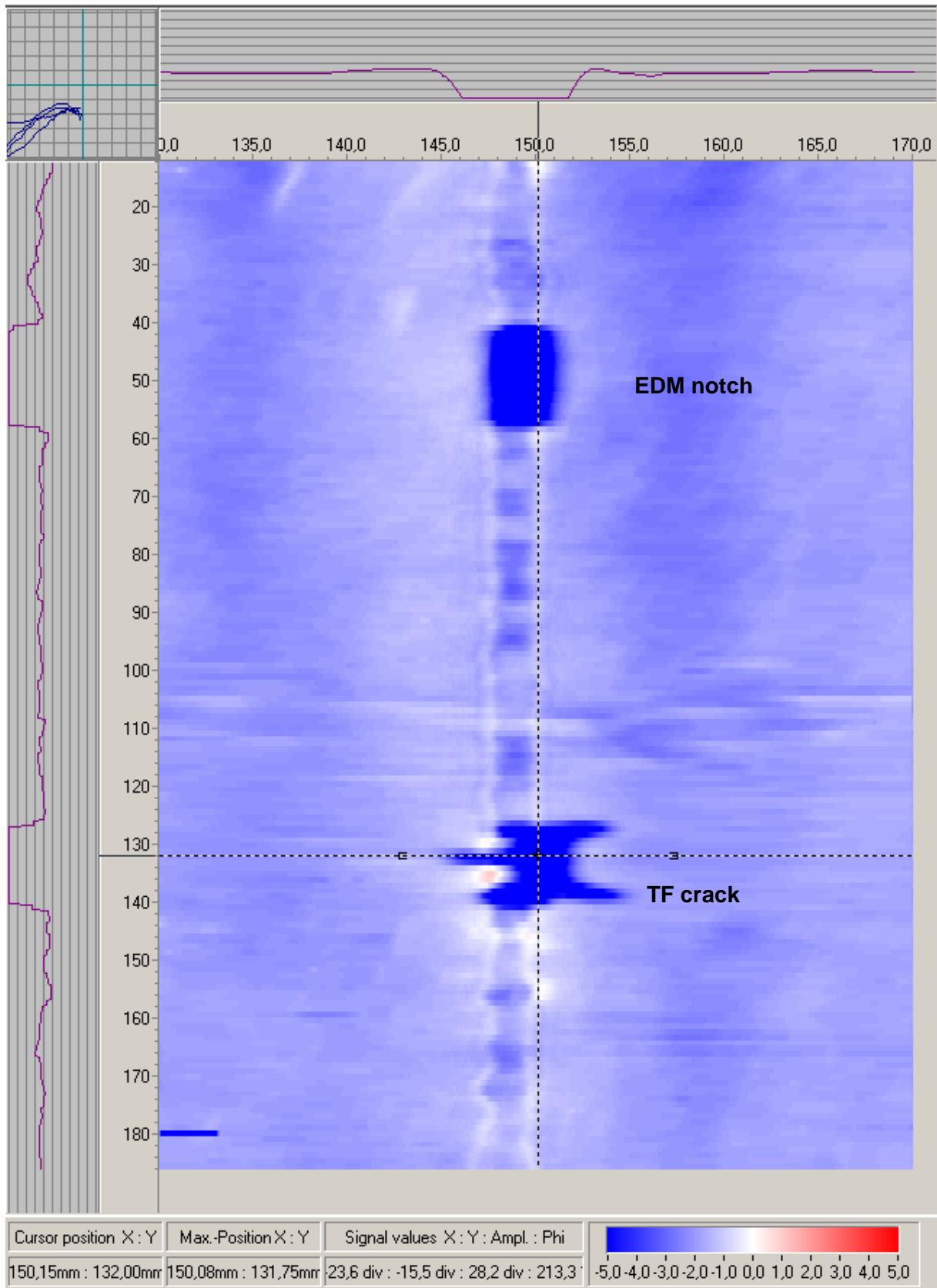


Figure 23 b. C scan of the test piece TF (Y-component), small diameter absolute probe A-T-TS10-F4, frequency 100 kHz, 20 dB additional gain was applied.

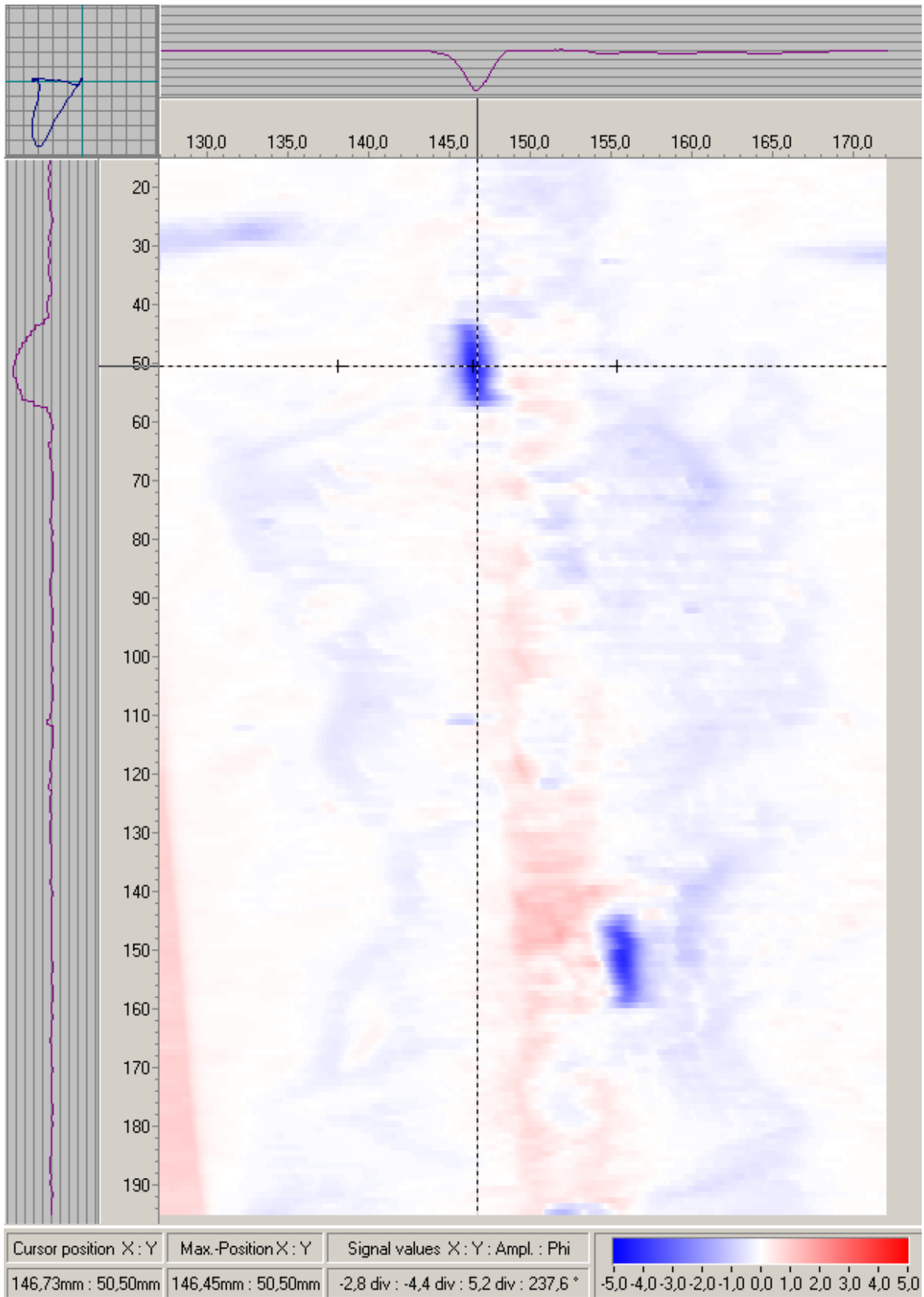


Figure 24a. C scan of the test piece MF (Y-component), small diameter absolute probe A-T-TS10-F4, frequency 100 kHz, 10 dB additional gain was applied for Y.

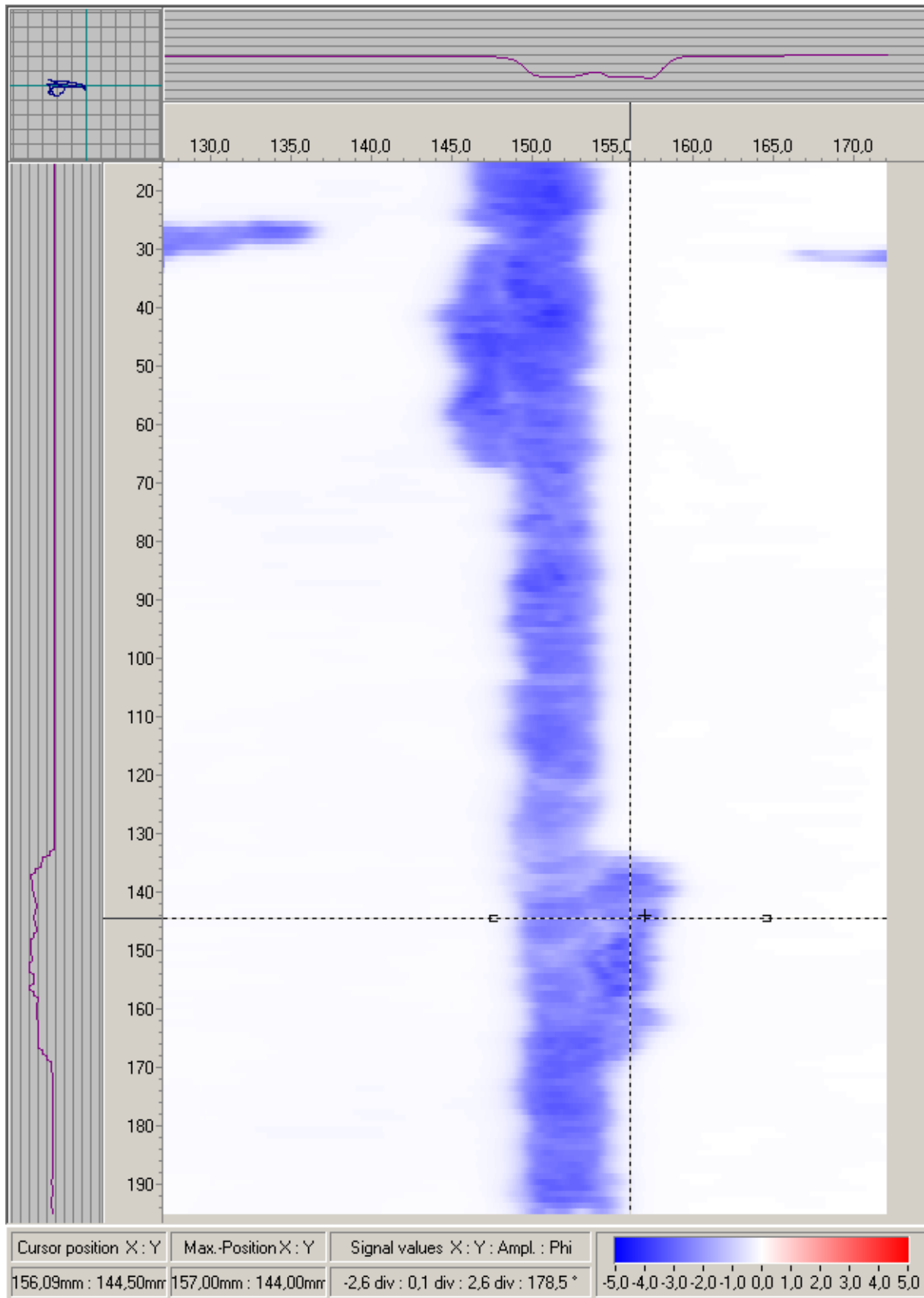


Figure 24 a. C scan of the test piece MF (X-component), small diameter absolute probe A-T-TS10-F4, frequency 100 kHz.

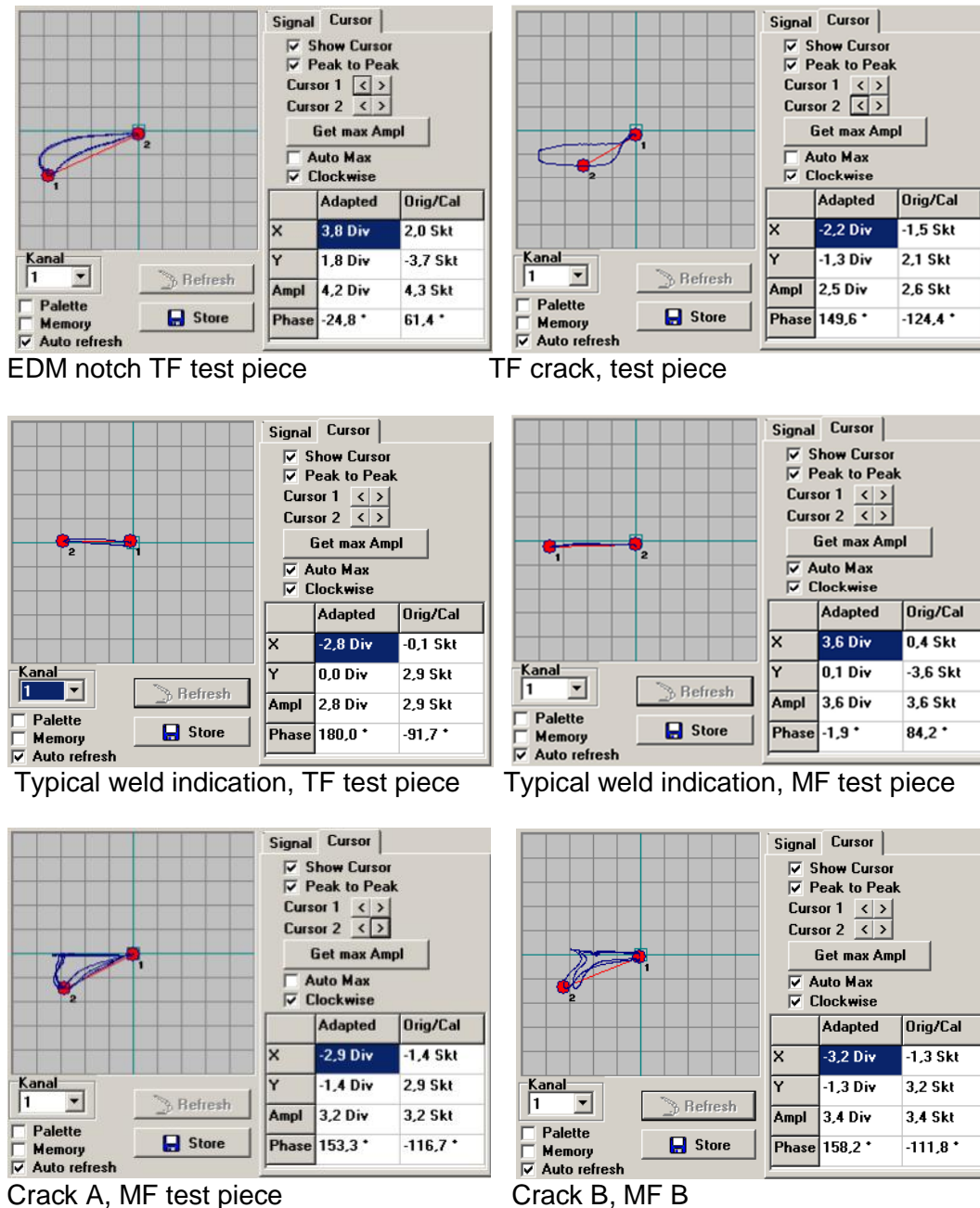


Figure 25. Impedance plane presentations of indications of a notch, fatigue cracks and welds in TF and MF test pieces, when A-T-TS10-F4 probe was applied, frequency 200 kHz.

The amplitudes of all indications of fatigue cracks and notches of the test pieces MF, TF, T284 and T285 recorded with the A-T-TS10-F4 are given in **Figure 26**. The applied frequency was 100 kHz. The amplitudes of the indications of 40 mm and 20 mm long notches were practically the same. The amplitude of the indication of the EDM notch (5 x 12 mm) in the weld of the TF piece was higher than that of the longer EDM notch (5 x 20 mm) in the test piece T285. The amplitude of the indication due to this 5 mm deep and 12 mm long notch was equal to the one of MF crack. The amplitude of the MF crack A was the highest of all crack indications.

The applied technique can be used to size defect lengths, but not to size the depths deeper than 2 mm due to the increasing saturation of the amplitude of the indications when the defect depth exceeds 2 mm.

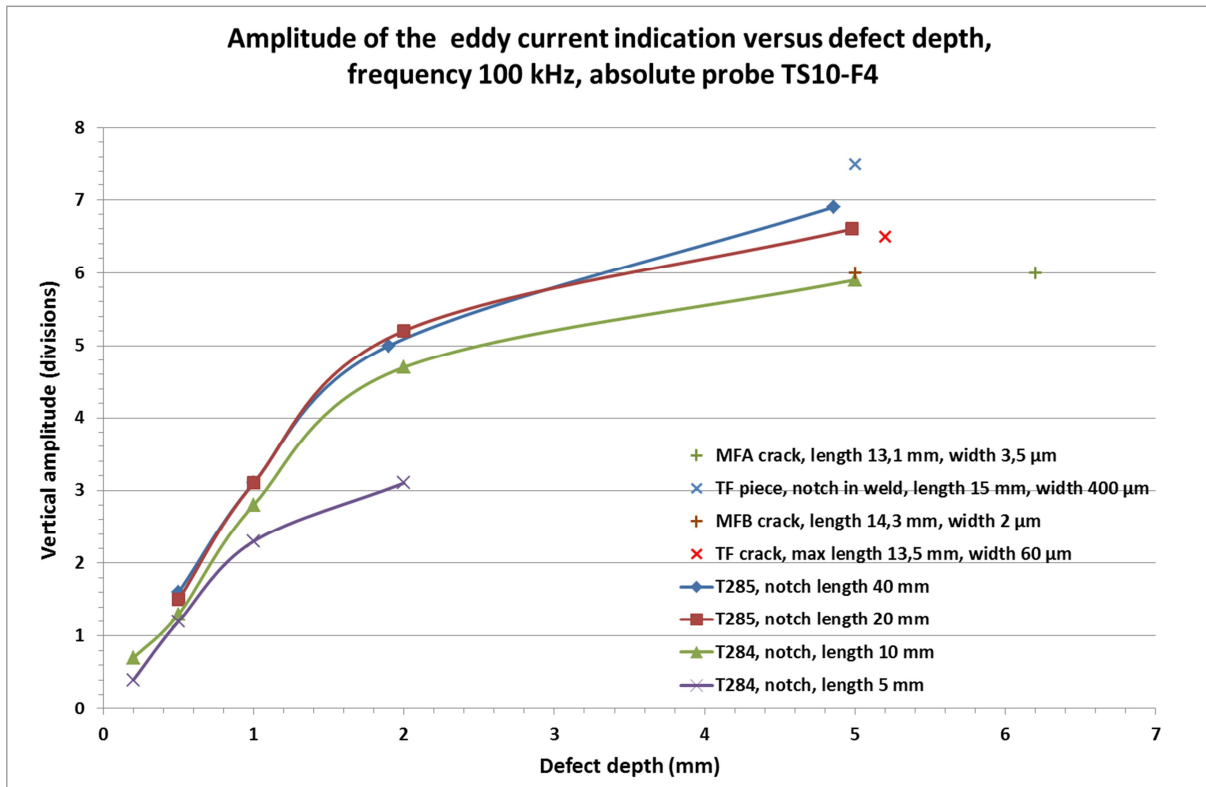


Figure 26. Amplitude of eddy current indications of TF and MF cracks and notches versus defect depth, when absolute probe A-T-TS10-F4 was used. The studied test pieces were TF, MF, T284 and T285. The eddy current frequency was 100 kHz.

Pencil probes can be used to size the length of the cracks. **Figure 27** shows the “ET lengths” of the three studied cracks and the EDM notch in the TF piece. Several different criteria can be applied when sizing the length of the crack. Here the full amplitude drop technique was used to size the crack lengths (blue dots in **Figure 27**). This sizing technique slightly oversized the length of the cracks. More accurate results will be achieved if $0.2 \times$ diameter of the probe dip is subtracted from the length measured with the full amplitude drop technique (green dots in **Figure 27**).

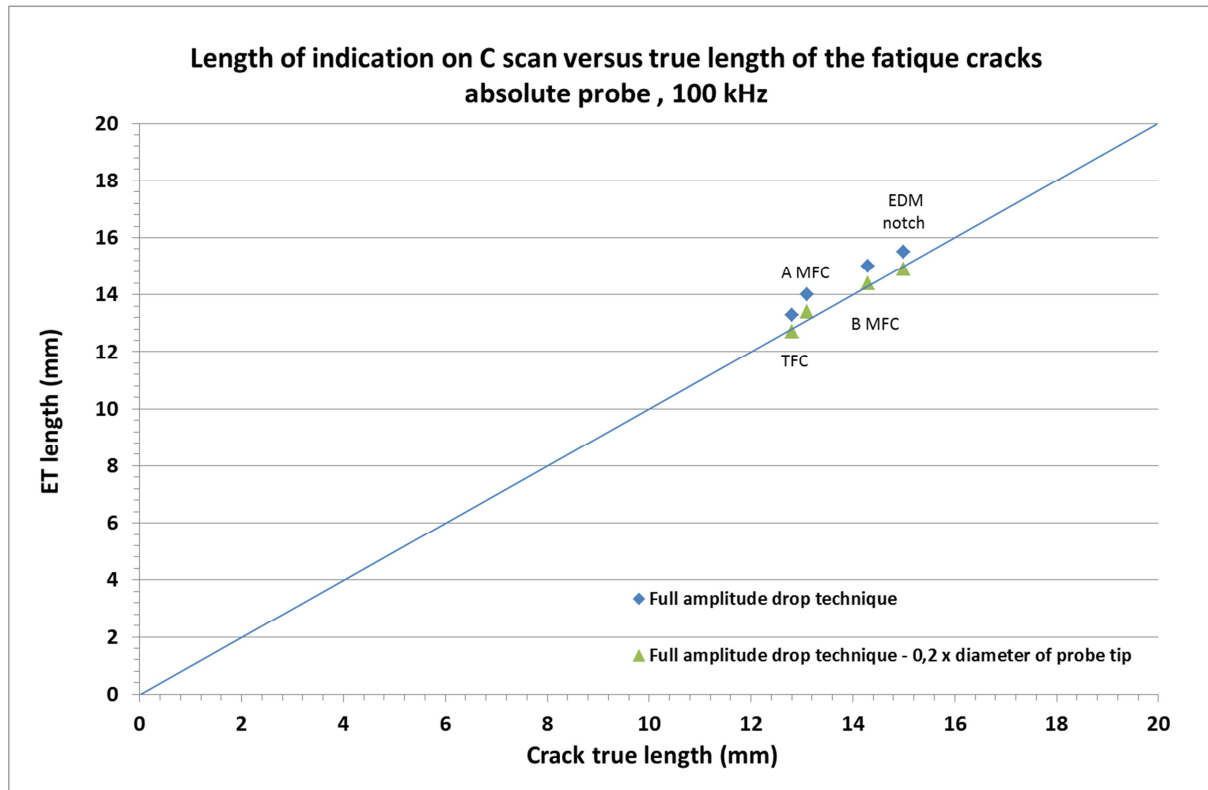


Figure 27. ET defect length versus true defect length of TF and MF cracks and an EDM notch, when absolute probe A-T-TS10-F4 was used. The eddy current frequency was 100 kHz.

6.3.4 Differential pencil probe

The TF test piece was scanned using differential probe TMT DP21 and 500 kHz frequency. The C scan is shown in **Figure 28**. In the C scan the Y component of the recorded eddy current signal is presented. The indications of the large notch and fatigue crack can be easily detected. Even all five side branches of TF crack can be seen. The crack, notch and weld indications are shown in **Figure 29**. The Y-coordinate of the amplitude of the TF crack indications exceeded the maximum weld indication by 16 dB. This technique was not used to scan the MF test piece due to higher noise around the MF cracks.

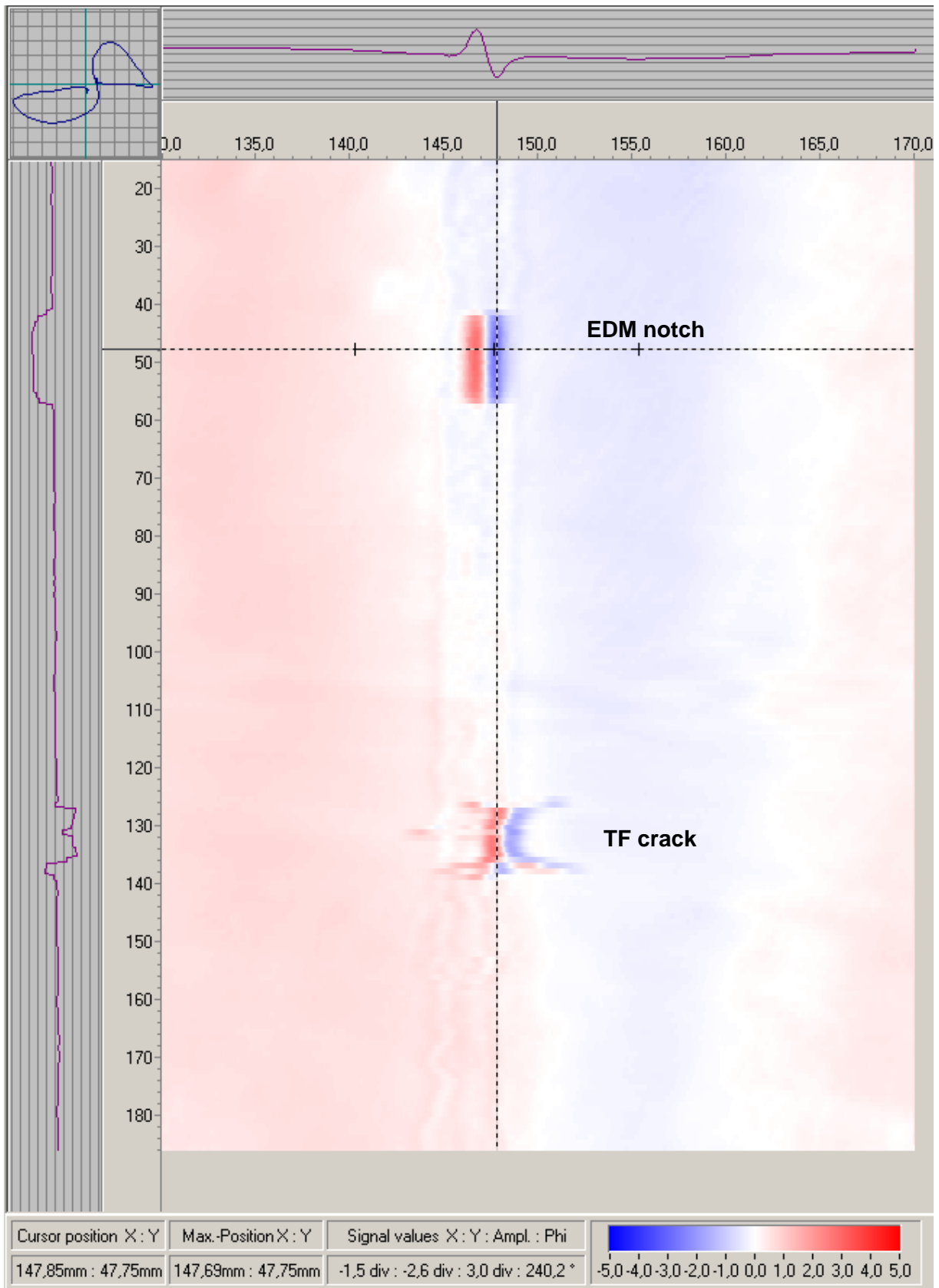


Figure 28. C scan of test piece TF (Y-component), small diameter differential probe A-T-TS10-F4, frequency 500 kHz.

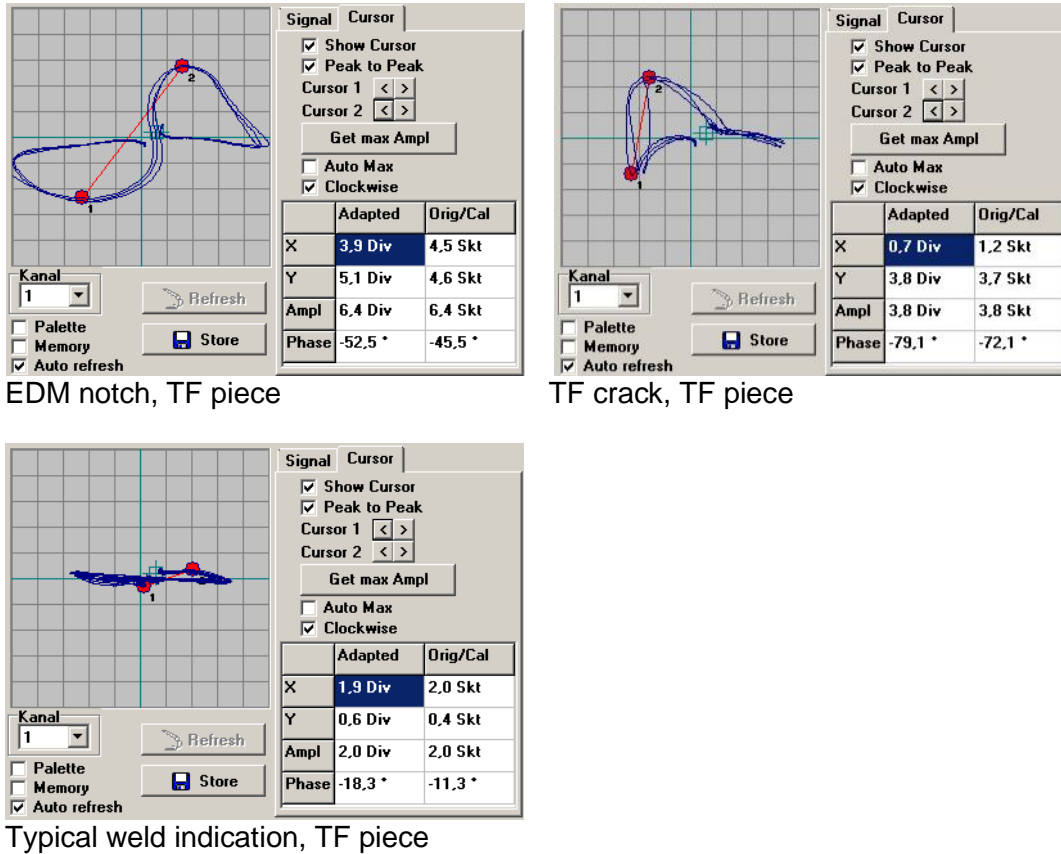


Figure 29. Impedance plane presentations of indications of a notch, fatigue cracks and welds in TF test piece, when differential pencil probe TMT DP21 was applied, frequency 200 kHz.

6.4 Simulation of eddy current testing

Simulation of eddy current testing (ET) with the probe SPO 2210 was applied to study more closely the effect of the defect depth and length on the amplitude of the eddy current indications. There are two axial parallel coils with ferrite cup core shields in the probe SPO 2210. In simulation the following parameters were used for the probe SPO 2210

- Coil outer diameter 11 mm
- Coil inner diameter 5 mm
- Coil height 2 mm
- Distance between the centre points of the coils 12 mm.

In simulation of the widths of the 1 mm, 2 mm, 5 mm and 10 mm deep notches were 60 μm , 100 μm , 200 μm and 400 μm respectively. In **Figure 30** there is an example where a family of solid curves present the measured amplitudes as a function of defect depth and a family of dotted curves present amplitudes generated in the ET simulation. The same results of measurements were presented also in **Figure 16**. The amplitudes of simulated indications were “calibrated” by using the measured amplitudes of 40 mm long notches. After “calibration” the amplitudes of simulated indications fit quite well with the measured amplitudes except in the case of 10 mm deep and 20 mm long notch. The reason for this deviation is not fully understood.

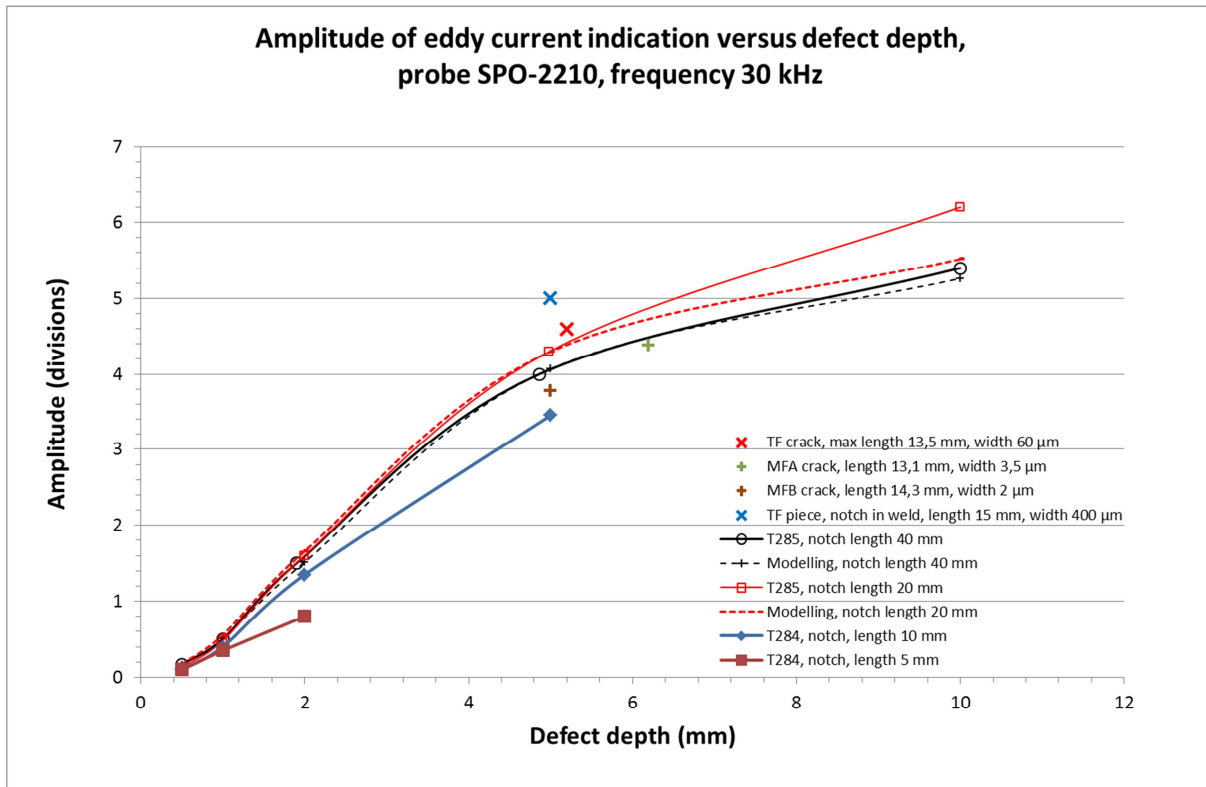


Figure 30. Amplitudes of measured and simulated eddy current indications of EDM notches versus defect depth, the measured amplitudes of TF and MF cracks are also included. Here the maximum length of MFA crack is given.

Figure 31 shows the amplitudes of measured and simulated indications of EDM notches as a function of defect length. There open marks present the true amplitudes of the indications of notches in the test pieces T284 and T285 and in test piece TF. The solid lines present the results of simulation (brown, black, red and blue lines). The results of simulation have been scaled using the amplitude of 40 mm long notches. The dotted lines present the interpolated values. In interpolation the values achieved by simulation were applied. Surprisingly the amplitudes of the indications have clear maximum, when the defect length is about 15 mm.

This kind of family of curves can be used to size the defect depth, if the length of the defect has been measured by small diameter pencil probe, see **Figure 27**. This is demonstrated in **Figure 32**, which includes a family of amplitude versus depth curves and the amplitudes and lengths of the TF crack and the two MF cracks.

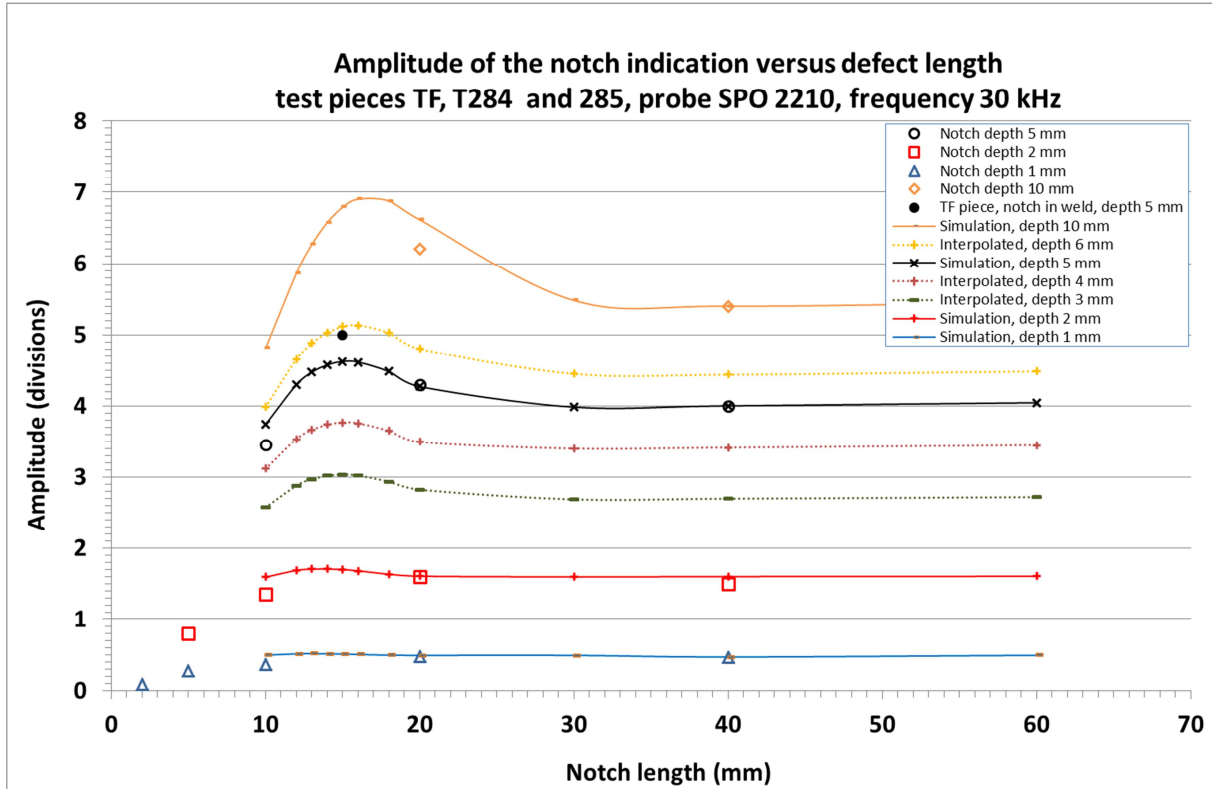


Figure 31. Open marks: the measured amplitudes of the indications due to notches of different length and depth. Solid lines: amplitude versus defect length calculated by Siva simulation program. Dotted lines: amplitude versus defect length interpolated values.

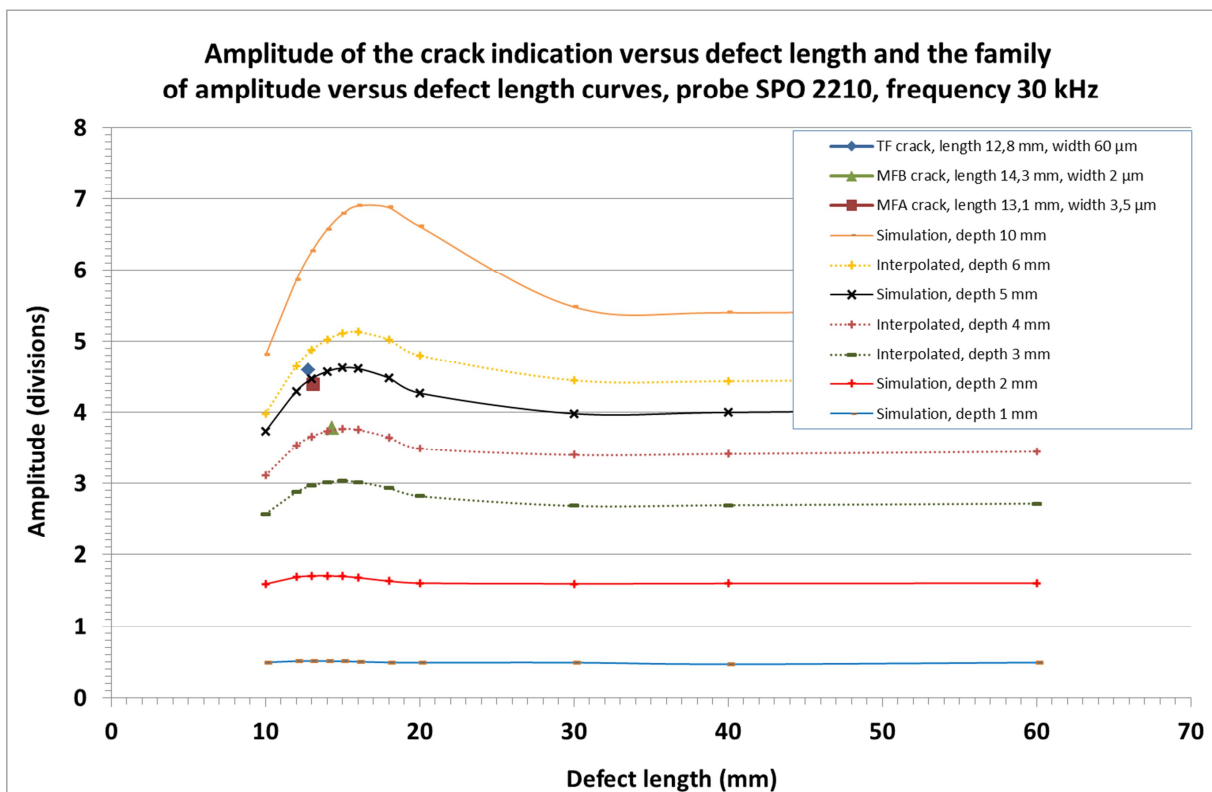


Figure 32. A family of amplitude versus defect length curves and the amplitude and the length of the studied TF and MF cracks.

6.4.1 Crack depth sizing with large ET probe

The results of measurements with the probe SPO 2210 and simulation of the measurement with the probe SPO 2210 in sizing the depths of the fatigue cracks are given in **Figure 33**. The depth of TF crack was estimated well in spite of the five side branches. The depths of the MF crack were underestimated about 20%. One reason for the underestimation might be the small opening of the MF cracks (3.5 μm and 2 μm) compared to the EDM notches used as reference defects. The width of EDM notches varied from 60 μm up to 440 μm depending on the depth of the EDM notch. The success in sizing of TF crack which was also narrow compared to EDM reference notches may be due the additional branches which may boost the eddy current indications of the TF crack.

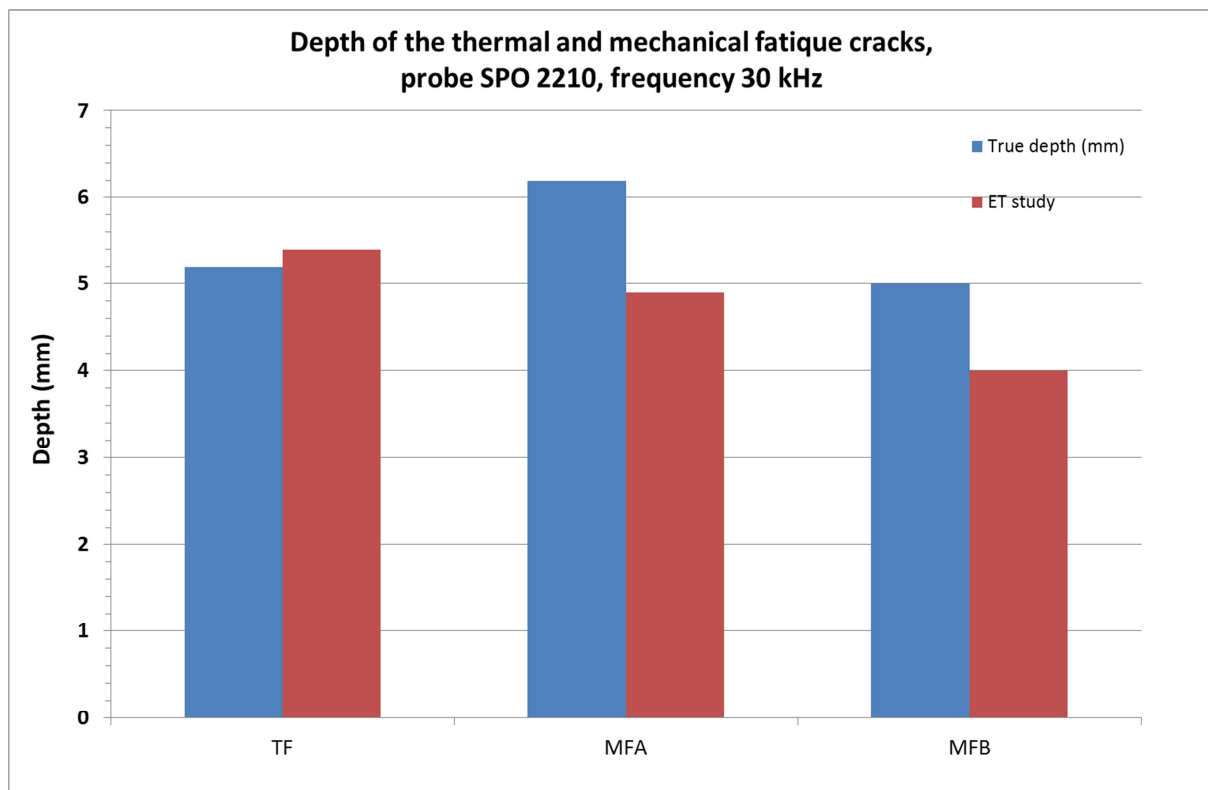


Figure 33. Estimated depth of TF and MF cracks, estimation is based on the length sized the absolute probe A-T-TS10-F4 and the amplitudes measured by the probe SPO 2210 (frequency 30 kHz) and amplitudes calculated by Civa simulation software.

7. Discussion

The surfaces of the test pieces were mostly planar and the roughness of the surface was small enough for eddy current testing purposes. However the area weld crowns and weld roots of the test pieces TF and MF were ground so that these areas were about 0.4 -0.6 mm below the general surface level of the test pieces as show in **Figures 3 and 4**. Even if this surface waviness did not induce any larger indications, it will attenuate amplitudes in the case of large size probes like SPO 2210 by increasing the distance between the surface of the test piece and the coils of the probe.

All cracks were in the root side of the test pieces. The cracks were open to the surface. The size of the cracks sizes was very near to the target value, depth 5 mm, length 15 mm. The opening displacement of the TF crack was about 60 μm . This is realistic opening displacement for the 15 mm long and 5 mm deep in service induced crack. Unfortunately TF crack had several branches. For this reason any general conclusions cannot be drawn from

the results of the TF crack. The opening displacement of the MF cracks was very small. The crack MFB was so tight, that it was not properly see by SEM. The surface length of the TF crack was slightly smaller than the maximum under surface length. The surface length (12.8 mm) was used in crack sizing. The EDM notch in TF piece seemed to locate quite near to the centre line of the weld, not in the solidification line of the weld as planned.

All defects were easily detected by ET with all applied techniques. Only the technique, where small diameter differential pencil probe was applied, had problems to detect the MF cracks. It is supposed that the local permeability changes due to the additional welds at the location of MF cracks were the reason to the increased material noise. The additional welds necessary to fabricate and implant the MF cracks were easily detected by the small diameter absolute pencil probe.

The error in length sizing was smallest when small diameter pencil probes were used. In length sizing the full amplitude drop technique was used. The applied eddy current transducer was the small diameter absolute pencil probe A-T-TS10-F4. The accuracy in length sizing was surprisingly good, see Figure 27. The best results were achieved after minor correction based on the diameter of the probe tip was conducted. The length error was only from -0.1 mm to 0.3 mm, when this correction was applied. The general shape of all cracks (and EDM notch) was similar (cracks were nearly semi-circular). The depth length ratio of the cracks varied from 2.1 to 2.86. The depth of the crack increased abruptly at the ends of the cracks. For this reason it was quite easy to locate the ends of the crack with high repeatability. This is main reason for the exceptional good length sizing result.

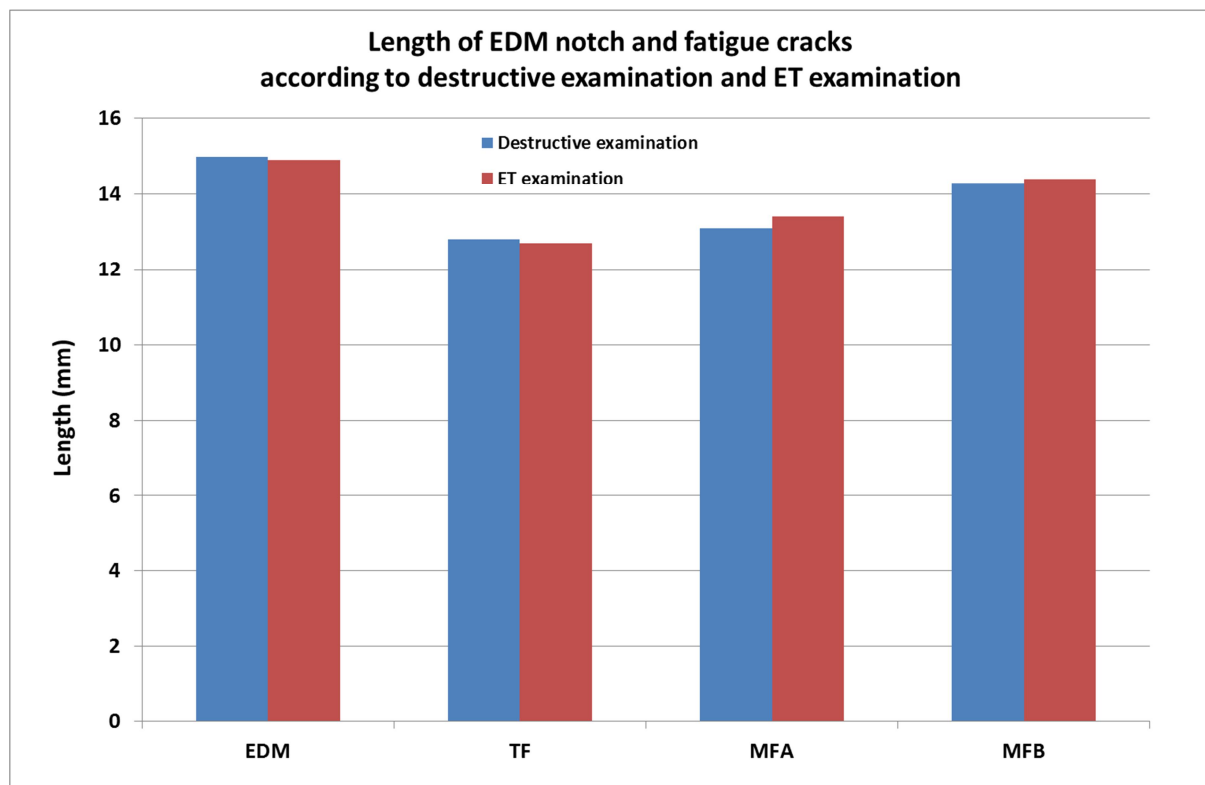


Figure 33. The DT and ET lengths of an EDM notch and three fatigue cracks, the full amplitude drop technique with correction was applied. The absolute pencil probe A-T-TS10-F4 was used. The eddy current frequency was 100 kHz.

Large size probes with deep penetrating eddy currents were successfully applied to size the depth of the studied deep fatigue cracks. Even the 5 mm and 10 mm deep notches were distinguished from each other with the probes SPO-2210 and SPO-1985. No saturation of eddy current indications of 10 mm deep defects was observed, when the largest probe SPO-1985 was used. The reference defects in the test pieces T284 and T285 and Civa simulation

software were used to generate the family of calibration graphs shown in **Figure 31 and 32**. The depths of the fatigue cracks were estimated using these graphs. As shown in **Figure 33** the accuracy in sizing the depth of TF crack was good in spite of the five side branches. The depths of the two MF crack were underestimated about 20% - 23%. One reason for the underestimation might be the small opening of the MF cracks (3.5 μm and 2 μm) compared to the EDM notches used as reference defects even if the opening of notches was taken into account in simulation. The width of EDM notches used to generate the calibration graphs varied from 60 μm up to 440 μm depending on the depth of the EDM notch. The deeper the notch the higher was the notch width. The success in sizing of TF crack, which was also narrow compared to EDM reference notches, might be due to the additional branches which may boost the eddy current indications of the TF crack.

The depth of the EDM notch in the root area of the weld in TF piece was clearly oversized (18 %). **Figure 23** and **28** show that the notch locates quite near to the middle line of the weld root. The reason for the over sizing might be the higher permeability of the weld material compared to the austenitic material of the blocks T284 and T285.

The effect of higher magnetic permeability of austenitic welds on the amplitudes of ET indications will be studied more closely. For that purpose new test pieces will be manufactured. The weld root and weld crown will be milled exactly to the same level than the base material to get rid of the changes due to the waviness of the surface of the weld zone. Several notches of same size will be machined in the weld and in the base material to be able to draw statistically reliable conclusions of the results of the study. The new study does not belong to the SAFIR2018 project WANDA (Nondestructive Testing of NPP Primary Circuit Components and Concrete Infrastructure).

8. Summary

Three fatigue cracks were fabricated in two austenitic test pieces. The cracks located in the solidification line of the weld to simulate surface breaking service induced cracks. One of the cracks was fabricated using thermal fatigue (TF). The other two cracks were fabricated using mechanical fatigue (MF). The size of the cracks was quite near to the target value, 5 mm x 15 mm (depth x length). The TF crack had several branches. The MF crack had no branches.

All relevant NDT methods and techniques were used to detect, to size and to characterize the cracks before destructive examination. The applied methods included: liquid penetrant, x-ray, ultrasonic, eddy current and SEM microscopy. Eddy current simulation was used to extend the family of "calibration graphs" used in defect depth sizing. In this study results of eddy current test and eddy current simulation are given.

All defects were easily detected by ET with all applied techniques. Only the technique, where small diameter differential pencil probe was applied, had problems to detect the MF cracks. It is supposed that the local permeability changes due to the additional welds at the location of MF cracks were the reason to the increased material noise. The location of additional welds necessary to fabricate and implant the MF cracks was easily detected by the small diameter absolute pencil probe.

The error in length sizing was smallest when small diameter absolute pencil probes were used. In length sizing the full amplitude drop technique was used. The accuracy in length sizing was surprisingly good. The length error was only from -0.1 mm to 0.3 mm. The general shape of all cracks (and EDM notch) was similar (cracks nearly semi-circular). The depth of the crack increased abruptly at the ends of the cracks. For this reason it was easier to locate the ends of the crack. This is main reason for the exceptional good length sizing result.

Large size probes were applied to size the depth of the studied fatigue cracks. Even the 5 mm and 10 mm deep notches were distinguished from each other with the probes SPO-2210 and SPO-1985. No saturation of eddy current indications of 10 mm deep defects was observed, when the largest probe SPO-1985 was used. The reference defects in the test pieces T284 and T285 and simulation were used to generate the family of calibration graphs. The accuracy in sizing the depth of TF crack was good in spite of the five side branches. The depths of the two MF cracks were underestimated (20% - 23%). One reason for the underestimation might be the small opening of the MF cracks (3.5 μm and 2 μm) compared to the EDM notches used as reference defects. The width of EDM notches used to generate the calibration graphs varied from 60 μm up to 440 μm depending on the depth of the EDM notch. Another reason for the underestimation might be the shape of the defects. The cracks were semi-circular and the notches were rectangular.

The depth of the EDM notch in the root area of the weld in TF piece was clearly oversized (18 %). The notch locates quite near to the middle line of the weld root. The reason for the over sizing might be the higher permeability of the weld material compared to the austenitic material of the reference pieces T284 and T285.

The effect of higher magnetic permeability of austenitic welds on the depth sizing capability of ET should be studied more closely. For that purpose new test pieces, where the weld root and weld crown are milled exactly to the same level than the base material to get rid of the sensitivity changes due to the waviness of the weld zone should be fabricated. Several notches of same size should be fabricated in the weld material and in the base material to be able to draw statistically reliable conclusions of the results of the study.

References

1. Esa Leskelä, Ari Koskinen, Jonne Haapalainen, Ulla Ehrnsten, Juha-Matti Autio, Comparison of artificial flaws in austenitic steel welds with NDE methods. Research report VTT-R-05649-14, 50 p
2. Esa Leskelä, Ari Koskinen, Comparison of mechanical and thermal fatigue cracks by ultrasonic examination. Research Report VTT-R-00626-14, 65 p
3. Jonne Haapalainen, Ultrasound simulation of fatigue flaws. Research Report VTT-R-00674-14, 10 p
4. Jonne Haapalainen, Ultrasonic simulation and simulation verification in demanding inspection applications. Research Report VTT-R-00846-13, 10 p
5. Antti Tuhti, Jonne Haapalainen, Work report on test of digital radiography Research Report VTT-R-00847-13, 7 p
6. Esa Leskelä, Ari Koskinen, Ultrasonic tests to compare mechanical and thermal fatigue cracks in 316L plates. Research Report VTT-R-00932-13, 70 p
7. Jäppinen, Tarja; Koskinen, Ari; Leskelä, Esa; Tuhti, Antti; Haapalainen, Jonne; Sandlin, Stefan. 2013. Monitoring of the structural integrity of materials and components in reactor circuit (MAKOMON). In: SAFIR2014. The Finnish Research Programme on Nuclear Power Plant Safety 2011-2014. Interim Report. Simola, Kaisa (ed.). VTT Technology 80. VTT, pp. 292 – 301 <http://www.vtt.fi/inf/pdf/technology/2013/T80.pdf>

8. Ehrnsten, Ulla; Pakarinen, Janne; Karlsen, Wade; Hänninen, Hannu; Mougnot, Roman; Soinila, Erno; Ahonen, Matias; Autio, Juha-Matti; Aaltonen, Pertti; Saukkonen, Tapio. 2013. Environmental influence on cracking susceptibility and ageing of nuclear materials (ENVIS). In: SAFIR2014. The Finnish Research Programme on Nuclear Power Plant Safety 2011-2014. Interim Report. Simola, Kaisa (ed.). VTT Technology 80. VTT, pp. 268 – 282 <http://www.vtt.fi/inf/pdf/technology/2013/T80.pdf>
9. Ari, Koskinen, Esa Leskelä, 2013. Differences in indications of different artificially produced flaws in non-destructive examination. The 10th International Conference on NDE in Relation to Structural Integrity for Nuclear and Pressurized Components, Cannes, France, 1-3 October 2013. COFREND (Confédération Française pour les Essais Non Destructifs) <http://www.ndt.net/index.php>